

Supporting information:
Fitness consequences of early life conditions and
maternal size effects in a freshwater top predator

Yngvild Vindenes^{*a}, Øystein Langangen^a, Ian J. Winfield^b and L.
Asbjørn Vøllestad^a

^aCentre for Ecological and Evolutionary Synthesis (CEES),
Department of Biosciences, University of Oslo, Oslo, Norway

^bLake Ecosystems Group, Centre for Ecology & Hydrology,
Lancaster, U.K.

Overview

Appendix S1: Additional information on the study system and model

Appendix S2: Estimation of vital rates from data

Appendix S3: Methods and additional results to sensitivity and elasticity analyses

^{*}yngvildv.vindenes@ibv.uio.no

Appendix S1: Additional information on the study system and model

In this appendix we provide some additional information on the study system and model, including A1) the observed temperature time series, A2) schematic overview of annual events in the life cycle, A3) histogram of the observed egg weights (i.e. average egg weight per female), A4) predicted annual offspring survival over the study period, A5) effects of previous and current temperature on offspring number, and A6) discretization of the IPM for numerical calculation.

S1-1. Temperature time series

The focal environmental variable of this study is the annual mean surface temperature (referred to as “temperature”; fig. S1.1). Three of the coldest years occurred in the early 60’s (1962, 1963, 1965), and much of this decade was below the average temperature ($\sim 10.5^{\circ}\text{C}$). The warmest years all occurred towards the end of the time series, indicating a warming trend (Winfield *et al.*, 2008).

The annual mean temperature is a coarse measure, but is still able to capture the impacts of temperature on annual vital rates. In reality, temperature influences the vital rates differently at different times during the year. For instance, growth is most influenced by summer temperature whereas fecundity is most influenced by temperature during late summer and autumn, when the eggs are developed. However, these seasonal effects are largely captured by the mean annual temperature, so instead of using many different temperature variables leading to a more complex model we chose to use the annual mean. Future models could easily be expanded to include more detail through seasonal temperature measures. Other temperature measures (e.g. growing degree days) could also be used, and lead to similar qualitative results.

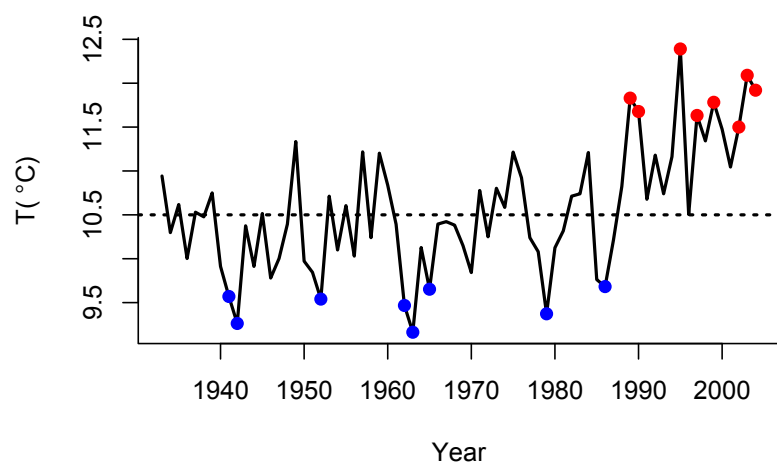


Figure S1.1: Annual mean surface temperature of the lake Windermere, indicating the coldest 10% and the warmest 10% of observations using blue and red dots, respectively. The horizontal line is the average temperature over the period ($\approx 10.5^{\circ}\text{C}$).

S1-2. Annual timing of events in the life cycle

Figure S1.2 shows an overview of the annual timing of life cycle and main sampling events in the study system. Since ovarian development (fecundity and egg weight) occurs mainly from October to March (Frost & Kipling, 1967), fecundity and egg weight may depend on the temperature in the year preceding the spawning year, T^* . Mortality and growth are assumed to occur primarily in summer, between spawning and the beginning of the ovarian development in autumn. In reality pike grow also during the winter months, but much slower than in the summer. Mortality in winter is also likely to be lower than in the summer month, because of less activity.

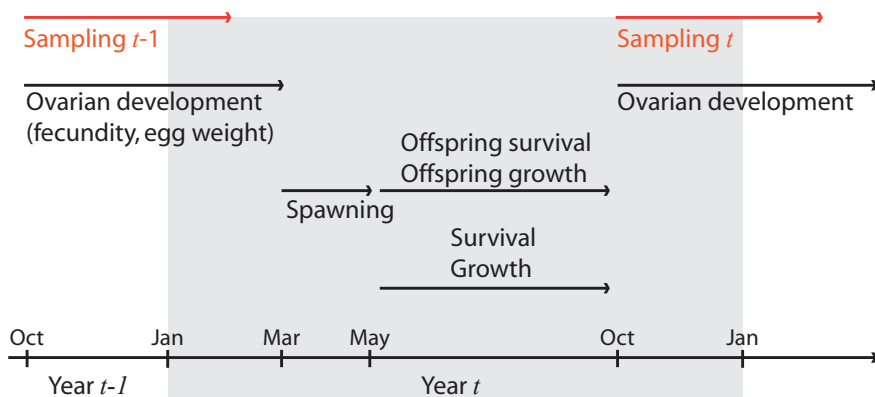


Figure S1.2: Overview of annual timing of life history events in the model, as well as the main sampling periods. Mortality and growth are assumed to occur primarily in summer, after spawning and before ovary development starts in autumn. Fecundity and egg weight may depend on the temperature conditions during the year preceding spawning, whereas the other vital rates may depend on the current temperature.

S1-3. Histogram of observed egg weights

Figure S1.3 shows a histogram of the observed egg weights for all females in the data set. The distribution is slightly positively skewed, with a mean of 0.00352 g, and a standard deviation of 0.000916. Over 95% of the data are within the interval 0.002-0.006g.

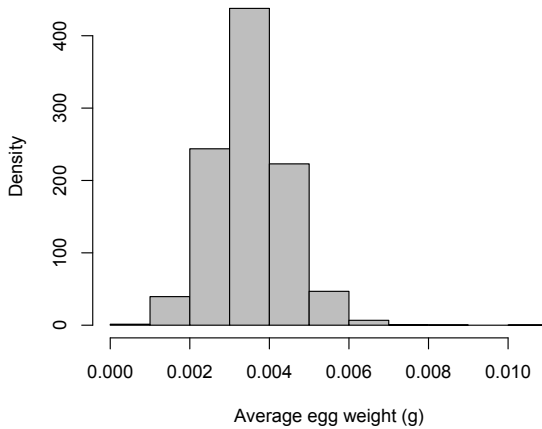


Figure S1.3: Histogram of the observed egg weights (3696 females, 1963-2003).

S1-4. Predicted offspring survival over the study period

Offspring survival (i.e., first year survival) could not be directly estimated from data, and four scenarios were developed for effects of temperature and egg weight. Here, we provide some predicted estimates of the annual offspring survival (fig S1.4), using the vital rate models together with the pike density estimates of Langangen *et al.* (2011). The pike are not susceptible to gillnet sampling until they are about 3 years of age, therefore we can only estimate the number of recruits at age 3 directly from the data (Paxton *et al.*, 2009; Langangen *et al.*, 2011). In this study, however, we are interested in first year survival (offspring survival), i.e. recruitment at age 1.

To obtain the predicted values for offspring survival, we first calculated the mean length at age using the growth model, for ages 2-9, assuming that all individuals start at the mean offspring length of $y = 23$ cm at age 1 (the temperature was assumed constant at 10.5°C). The mean length at age was then used to calculate the mean fecundity and survival at age. For each year, the mean fecundity was multiplied by the estimated density of the corresponding age class to obtain an estimate of the total number of eggs produced by the stock, M_t (this number was multiplied by 0.5 to obtain the number of female offspring). The number of eggs produced by a stock in a given year t result in a number of 3-year old pike three years later, R_{t+3} . The predicted average survival was 0.037 from age 1 to 2, 0.48 from age 2 to 3. Letting offspring survival be denoted as s_t , we then have the relationship $M_t s_t \cdot 0.037 \cdot 0.48 = R_{t+3}$. Thus, a rough estimate (prediction) of s_t is given by $\frac{R_{t+3}}{0.0177M_t}$.

Figure S1.4 shows this predicted offspring survival for each year of the time series. These predictions are made under the assumption that all the variability in recruitment at age 3 occurs during the first year, and therefore probably overestimates the variance in first year survival (a conservative measure). The predicted mean offspring survival was 0.00028. Most predicted values lie within the range 0.0001-0.0006 (one estimate is above and two below, Fig.S1.4), indicating that the variability in offspring survival (and in particular, the variability explained by temperature and egg weight) is likely lower than in our most extreme scenarios used in the main model. The maximum value is about 18 times higher than the minimum, but this includes all sources of variability.

Based on a least squares regression analysis with the predicted offspring survival as a response variable, there was a significant negative effect of total egg number the previous year, i.e. the egg number giving rise to the offspring at age 1 ($n = 53$, $t = -3.894$, $p = 0.000288$), and a positive effect of temperature dur-

ing the first year of life ($n = 53$, $t = 3.152$, $p = 0.002713$). This temperature effect was about 2.5 times weaker than the effect we assumed in scenario 3 of the IPM. The negative effect of egg number indicates an effect of within-cohort density regulation, but this was not considered further in this study.

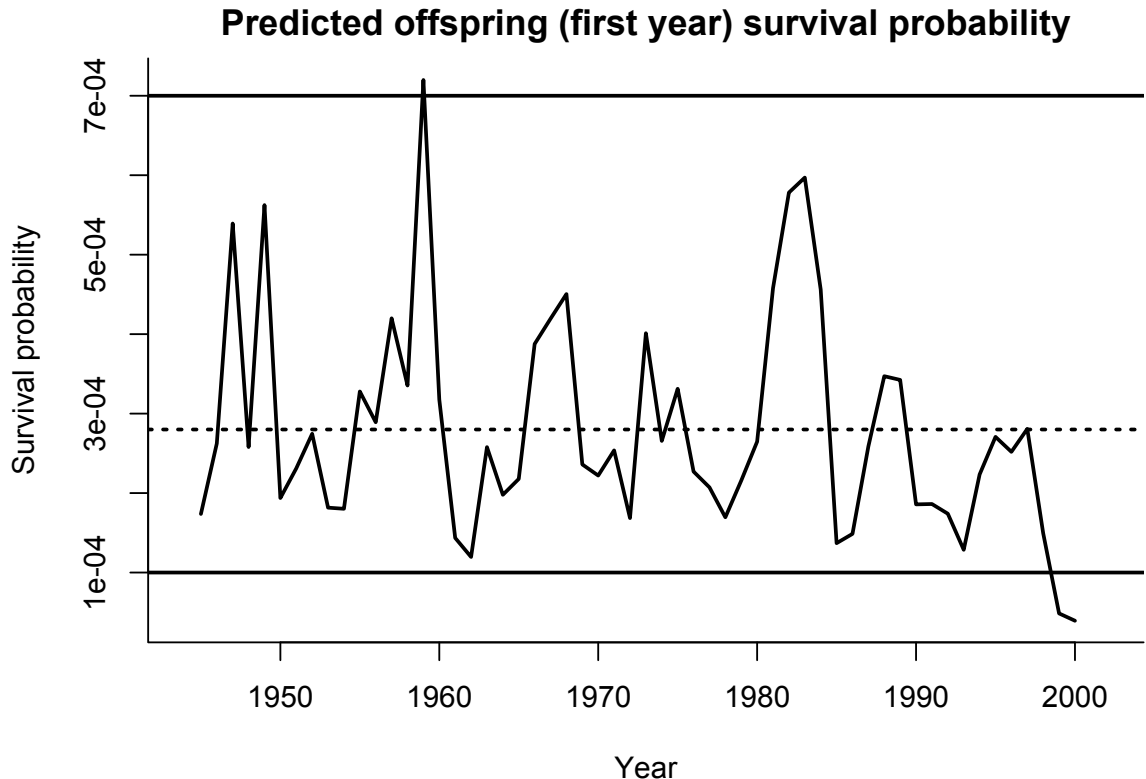


Figure S1.4: Predicted first year survival over the study period, using the vital rate models together with pike density estimates for different age classes. These calculations were made assuming no variance in second and third year survival probability. The dashed line corresponds to the mean 0.0028. Most values lie within the range 0.0001-0.0007 (solid horizontal lines).

S1-5. Effects of current and previous temperature on offspring number

In the main analysis temperature conditions were assumed to be constant over time (although evaluated at different levels). Here, we show how the offspring number

predicted from the model depends on current and previous temperature when the two are different. The previous temperature T^* affects egg weight, whereas current temperature potentially affects offspring survival, depending on the scenario for offspring survival (described in the main text).

Figure S1.5 shows how the estimated offspring number $b(x, T, T^*)$ as a function of length changes with different combinations of previous and current temperature, for each of the four scenarios of offspring survival. The most complex temperature effects are found for Scenario 1 with the negative interaction between current temperature and egg weight on offspring survival. If the current temperature is high, the effect of previous temperature on offspring number is small (Fig. S1.5). However, if the current temperature is low, so that offspring from larger eggs have a higher survival, the offspring number is much higher if the previous temperature was also low, leading to more large eggs being produced. Correspondingly, for this scenario the smallest offspring number is found for the combination of a high previous temperature and a low current temperature.

S1-6. Discretization of the IPM for numerical calculations

IPMs are typically discretized to a (large) matrix model before model calculations are done, so that the continuous projection kernel becomes a large projection matrix (Easterling *et al.*, 2000; Ellner & Rees, 2006; Merow *et al.*, 2014; Rees *et al.*, 2014). Note that the discretization of an IPM occurs after the vital rates have been estimated (Ellner & Rees, 2006). The number of mesh points determines the accuracy of the model calculations, for this model current length x (ranging from 10-130 cm) was discretized to a vector of 100 values, whereas offspring length y (ranging from 10-40 cm) was discretized to a vector of 25 values. The resulting projection matrix was then of dimension 2500×2500 .

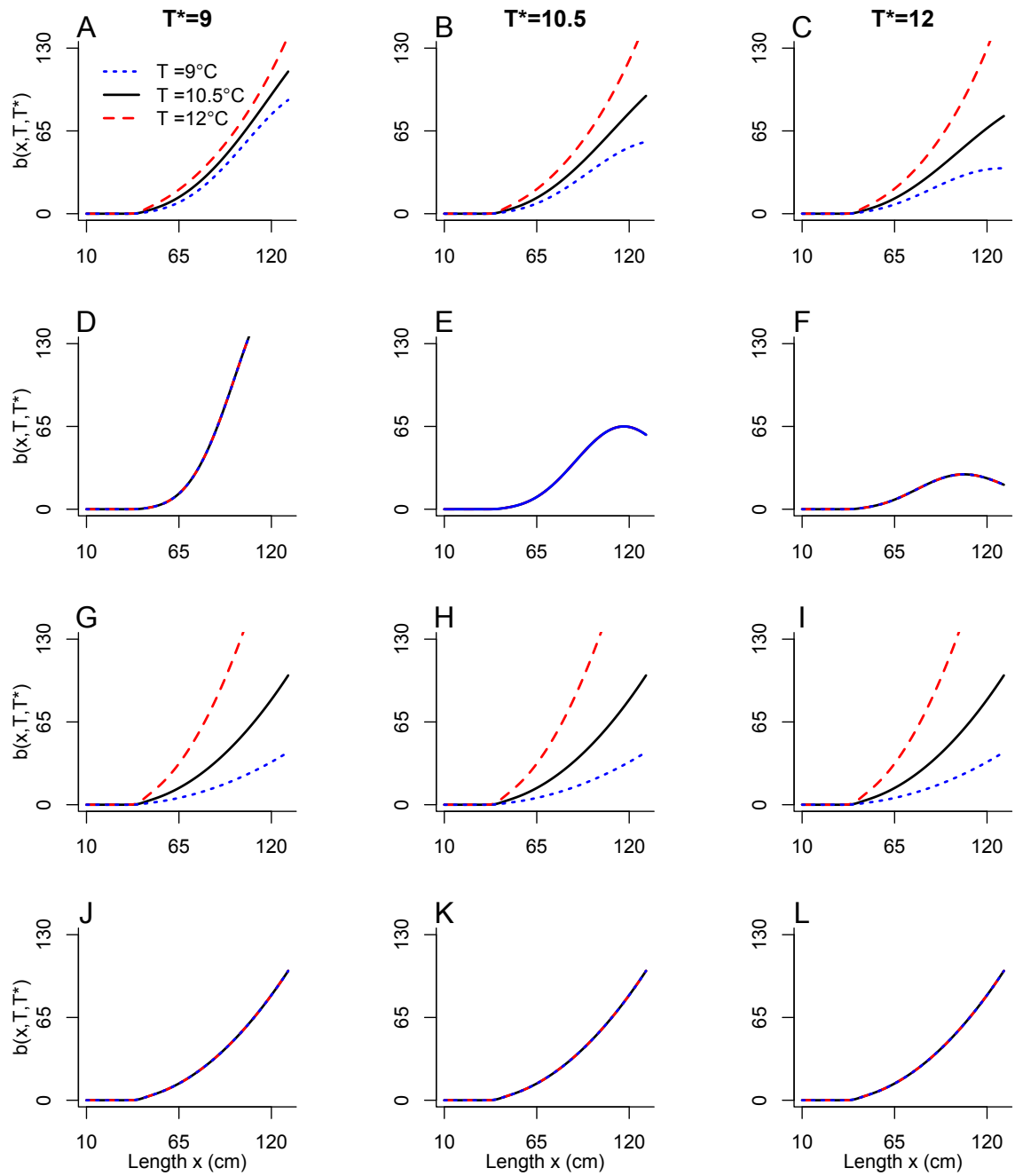


Figure S1.5: Offspring number $b(x, T, T^*)$ as a function of female current length x , for different values of current temperature T (within each panel) and previous temperature T^* (columns, as indicated). Each row represents one of the four scenarios for egg survival (Scenario 1: A-C, Scenario 2: D-F, Scenario 3: G-I, Scenario 4: J-L).

Appendix S2: Estimation of vital rates from data

In this appendix we provide more detailed information on the vital rate functions that determine survival, growth, and fecundity, including the statistical estimation. We also discuss how certain aspects of the vital rate models used here differ from earlier studies on the same population (Edeline *et al.*, 2007; Vindenes *et al.*, 2014; Vindenes & Langangen, 2015).

The vital rates estimated using mixed effects models were i) fecundity $m(x, T)$; ii) average egg weight $w(x, T)$, iii) the mean and variance of offspring length y' , $\mu_1(T)$ and σ_1^2 , respectively; and iv) the mean and variance of next year's length x' , $\mu_G(x, y, T)$ and $\sigma_G^2(x)$, respectively. Survival probability $s(x, y, T)$ was estimated using the Monte Carlo sampling method of Vindenes *et al.* (2014), updated to include the current growth model. All models included year as a random effect, in order to capture year-to-year random variation in the vital rates. Some models also included a fixed year effect in order to capture temporal trends not explained by the other covariates considered (see specific details for each vital rate below).

Model selection for the fixed effects was based on AICc comparison of candidate models estimated using maximum likelihood. The model fitting was done using the packages “nlme” (Pinheiro *et al.*, 2013) and “MuMIn” (Bartoń, 2013) in R (R Development Core Team, 2013). For each vital rate different candidate models were fitted and the model with the lowest AICc value was used for the IPM if the second highest ranked model had a $\Delta AICc > 2$. Otherwise, we selected the model with the fewest parameters among the candidate models within $\Delta AIC < 2$. Candidate models were fitted using maximum likelihood estimation, and final models were refitted using restricted maximum likelihood. Model fit was assessed using diagnostic plots (residuals against fitted values, residuals against each covariate, autocorrelation function for the residuals, and plots of the random year effects).

In the following we describe the estimation procedure for each vital rate.

S2-1. Fecundity

The model for fecundity $m(x, T)$ was fitted on a square root scale. The square root transformation is often used for count data and in this case the square root of fecundity was an approximately linear function of female current length (in contrast to the logarithm). All candidate models considered included year as a random effect and an exponential variance function with length as a covariate. The fixed effects structure was evaluated by AICc comparison of candidate models. The models for fecundity and egg weight included a somatic condition index among the covariates, as this had previously been found to have a positive effect on fecundity (Edeline *et al.*, 2007). Following a method developed for perch (Le Cren, 1951) the index was defined by Edeline *et al.* (2007) as $C = 100SM/SM_{std}$, where SM is the somatic mass (total mass - gonad mass) of a female pike with length x , and SM_{std} is the predicted somatic mass based on the population mean according to the equation $\ln(SM) = -6.59 + 3.44 \ln x$, fitted by least squares regression ($n = 3695$, $R^2 = 0.96$).

The global model for the fixed effects was given by

$$\sqrt{m(x, y, T)} \sim x + y + Y_r + T + C + M_o + Y_r^2 + xT + xY_r$$

where x is female current length, y is the offspring length (length at age 1), Y_r is year, T is temperature, C is the somatic body condition index defined above, and M_o is the month number (where January is numbered 13 and February 14, so that within each capture season from October to February M_o is an increasing variable). The candidate models considered were all all possible combinations of the covariates (interaction effects were not included without also including the

respective main effects). Initially only a linear fixed year effect was included in the fecundity model. However, plots of the random year effects then revealed a non-linear (quadratic) pattern. Therefore, we also included a fixed quadratic year effect to capture this non-linear temporal trend.

Table S2.1 shows the model selection table for the highest ranked candidate models. The three highest ranked models (within $\Delta AICc = 2$) did not include offspring length (y), so this covariate was not included in the final model. Among these, the model with the fewest covariates also excluded temperature. Table S2.2 shows the resulting fixed effects for the selected final model (model 3 excluding temperature and offspring length), which was refitted using restricted maximum likelihood.

Table S2.1: Model selection table for fixed effects in the fecundity model, modeled on a square root scale, showing the highest ranked candidate models based on AICc. Covariates considered were current length x , length at age 1 y , somatic condition index C , month M_o , year Y_r , and temperature T . All candidate models included year as a random effect and an exponential variance function with length as a covariate. Model 3 was used for the IPM.

Model	x	y	C	M_o	Y_r	T	Y_r^2	xY_r	xt	df	logLik	AICc	$\Delta AICc$	Weight
1	*	*	*	*	*	*	*	*	*	12	-17777	35578.9	0.00	0.333
2	*	*	*	*	*	*	*	*	*	11	-17779	35579.9	0.98	0.204
3	*	*	*	*	*	*	*	*	10	-17779	35580.0	1.15	0.188	
4	*	*	*	*	*	*	*	*	*	13	-17777	35580.9	2.01	0.122
5	*	*	*	*	*	*	*	*	*	12	-17779	35581.9	3.00	0.074
6	*	*	*	*	*	*	*	*	*	11	-17780	35582.1	3.16	0.069
7	*	*			*	*	*	*	*	11	-17783	35587.7	8.75	0.004
8	*	*			*	*	*	*	*	10	-17784	35588.5	9.60	0.003
9	*	*			*		*	*	*	9	-17785	35588.7	9.77	0.003
10	*	*	*	*	*	*	*	*	*	12	-17782	35589.7	10.76	0.002

In the fecundity model used in the main analysis the effects of year, month and somatic condition were kept constant equal to their mean (year 1982, month 11.4, and somatic condition 100). Figure S2.1 (left panel) shows how the observed mean number of eggs (across all individuals) changes with year and capture month, indicating an apparent increasing trend in fecundity over the study period. How-

Table S2.2: Effects and statistical significance (marginal tests) for the final fecundity model $\sqrt{m(x, T)}$ used in the IPM (model 3 from table S2.1, re-fitted using restricted maximum likelihood). The variance of the random year effect is 94.32, the residual variance is 5.87, and the estimated parameter for the exponential variance function is 0.0348. In the main analysis year was kept constant to 1982, month to 11.4, and somatic condition to 100.

Fixed effect	Estimate (SE)	F-value (denDF)	p-value
(Int)	$-3.63 \cdot 10^5$ ($5.06 \cdot 10^4$)	51.42 (3651)	<0.0001
x	$-8.15 \cdot 10$ ($1.07 \cdot 10$)	58.23 (3651)	<0.0001
Mo	1.63 ($4.98 \cdot 10^{-1}$)	10.74 (3651)	0.0011
C	$7.90 \cdot 10^{-1}$ ($4.65 \cdot 10^{-2}$)	284.25 (3651)	<0.0001
Y_r	$3.69 \cdot 10^2$ ($5.11 \cdot 10$)	52.2 (38)	<0.0001
Y_r^2	$-9.40 \cdot 10^{-2}$ ($1.29 \cdot 10^{-2}$)	53.12 (38)	<0.0001
xY_r	$5.43 \cdot 10^{-2}$ ($5.39 \cdot 10^{-3}$)	70.77 (3651)	<0.0001

ever, when other effects (such as length) were accounted for, the year effect was non-linear (Fig. S2.1, right panel) with an initial increase followed by a decrease, such that the difference between the beginning and end of the time series is not large.

Edeline *et al.* (2007) used the same data to study changes in reproductive investment over the study period. Their fecundity model and regression analysis differed in a few aspects from the model used here. In particular there was no effect of month, and only a linear fixed year effect was included. In addition, age was included as a covariate and fecundity was modeled on a log scale. The choice of log vs. square root scale does not have a large effect on the resulting final model. We obtained similar results using a model for fecundity estimated on log scale, but since the log of fecundity was not a linear function of length this would then require including a second order length effect. Fecundity models on a log scale (including a second order length effect) and square root scale look very similar except for the very largest individuals, where the model on square root scale predicts increasing fecundity with length whereas with the model on log scale the predicted fecundity

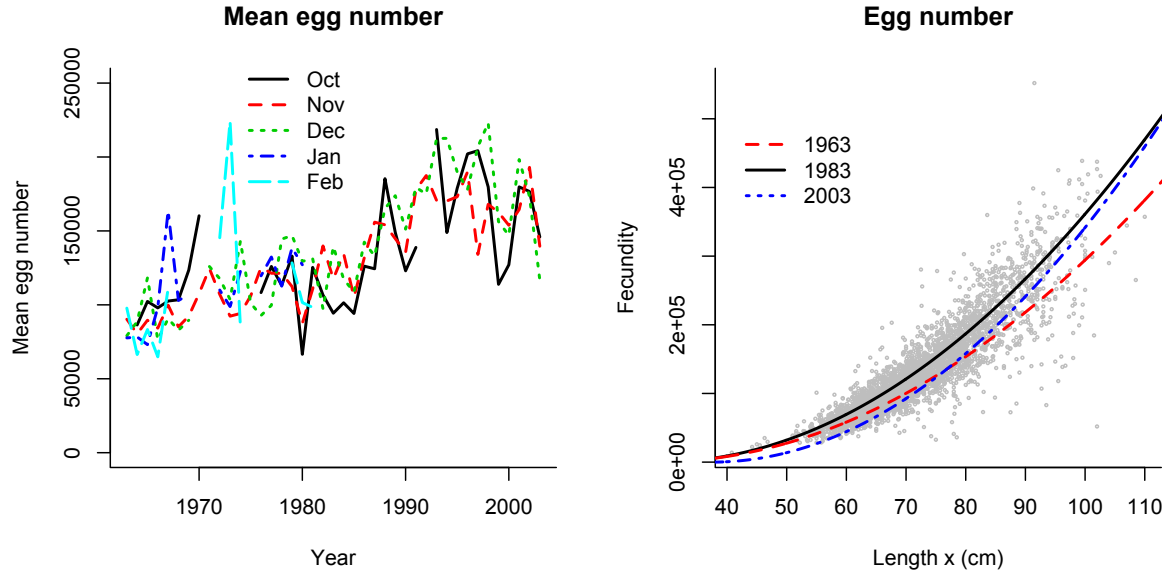


Figure S2.1: Left panel: Observed trends in the mean fecundity (for all individuals) across year and capture month. Right panel: Predicted effect of length on fecundity in the final model, for three different years.

levels off here. For the analysis this has only minor consequences as the proportion of large individuals in the population is so small.

We did not include age as a covariate because it is highly correlated with length. However, the final model on a square root scale (tables S2.1, S2.2) lead to practically the same predictions of fecundity as a function of length as a model on log scale that included age as well. Because the logarithm of fecundity is not a linear function of length, the non-linearity on log scale may have been captured by including age as a covariate, since data from fish at different ages span different length ranges. The lack of a significant month effect in the model of Edeline *et al.* (2007) is likely due to month not being included as an increasing variable within sampling year in that study, but the month effect on fecundity is quite small also in our final model (table S2.2).

Edeline *et al.* (2007) also reported a negative trend in fecundity over time (a linear year effect) and suggested that this could be explained by a rapid evolutionary response to harvesting. The non-linear year effect in our final fecundity model suggests that fecundity at a given length actually increased at first over the study period, before decreasing again (figure S2.1, table S2.2). An evolutionary response to fishing pressure is not a likely explanation for this non-linear trend.

The fecundity model used by Vindenes *et al.* (2014) also differed slightly from the model used here. It did not include a quadratic year effect, as it was estimated with data from 1968-2003 (not from 1963 as here) that did not capture the initial increasing trend. It also included a weak temperature effect, whereas the final model selected for this study did not include any temperature effects.

S2-2. Egg weight

As for the fecundity model, all candidate models considered for egg weight $w(x, T)$ included year as a random effect and an exponential variance function with length as a covariate. In addition, an ARMA(1,1)-model (autoregressive moving average of order $p = 1$, $q = 1$) was included to account for some temporal autocorrelation in the residuals, which was revealed by the diagnostic plots. The global model for the fixed effects was given by

$$w(x, y, T) \sim x + y + Y_r + T + C + M_o + x^2 + Y_r^2 + xT + XY_r,$$

where the variables are the same as defined for the fecundity model. We could not fit all possible candidate models when the autocorrelation structure was included (due to computation time). Therefore, we first did a preliminary model selection by fitting candidate models without including the autocorrelation structure for the

residuals, where all combinations of the covariates were considered. The highest ranked models among these (models having an Akaike weight > 0.0001) were then refitted including the autocorrelation function and a new model selection was done. In this case including the correlation structure did not affect the model ranking.

Table S2.3 shows the model selection table for the candidate models. The highest ranked model was the global model, whereas the second highest ranked model, where y was excluded, had a $\Delta AICc = 1.34$. Whenever included, the effect of y was negative but small. As the statistical support for including this effect was very weak, we selected the second highest ranked model for the IPM. Table S2.4 shows the resulting estimated fixed effects for this final model.

Table S2.3: Model selection table for fixed effects in the egg weight model, showing the highest ranked candidate models based on AICc. Covariates considered were current length x , length at age 1 y , temperature T , year Y_r , month M_o , and somatic condition index C . All models included year as a random effect, an exponential variance function with length as a covariate, and an ARMA(1,1) model to account for autocorrelation in the residuals. Candidate models were estimated using maximum likelihood.

Model	x	y	C	M_o	Y_r	T	x^2	Y_r^2	xT	xY_r	df	logLik	AICc	$\Delta AICc$	weight
1	*	*	*	*	*	*	*	*	*	*	16	22794	-45555.4	0.00	0.638
2	*	*	*	*	*	*	*	*	*	*	15	22792	-45554.0	1.34	0.327
3	*	*	*	*	*	*	*	*	*	*	15	22789	-45548.8	6.54	0.024
4	*	*	*	*	*	*	*	*	*	*	14	22788	-45547.2	8.18	0.011
5	*	*	*	*	*	*	*	*	*	*	13	22775	45523.8-	31.62	0.000

In the egg weight model used in the main analysis the effects of year, month and somatic condition were kept constant equal to their mean (year 1982, month 11.4, and somatic condition 100). Figure S2.2 shows the observed mean egg size as a function of sample year and month. The apparently negative linear trend in egg weight over the time period is largely explained by differences in sampling month.

As for the fecundity model, the final egg weight model also differed in a few aspects from that of Edeline *et al.* (2007). First, Edeline *et al.* (2007) found a

Table S2.4: Effects and statistical significance (marginal tests) for the final egg weight model $w(x, T)$ used in the IPM (model 2 from table S2.3, re-fitted using restricted maximum likelihood. The variance of the random year effect was $7.70 \cdot 10^{-13}$, the residual variance was $9.93 \cdot 10^{-8}$, and the estimated parameter for the exponential variance function was 0.0116. The parameters of the ARMA(1,1)-model were 0.9858 for the AR-parameter, and -0.8124 for the MA-parameter. In the main analysis year was kept constant to 1982, month to 11.4, and somatic condition to 100.

Fixed effect	Estimate (SE)	F-value (denDF)	p-value
(Int)	6.07 (1.78)	11.65 (3648)	0.0006
x	$-1.20 \cdot 10^{-3} (2.77 \cdot 10^{-4})$	18.63 (3649)	<0.0001
x^2	$-6.15 \cdot 10^{-7} (7.74 \cdot 10^{-8})$	63.21 (3649)	<0.0001
M_o	$4.51 \cdot 10^{-4} (2.50 \cdot 10^{-5})$	324.84 (3649)	<0.0001
C	$9.56 \cdot 10^{-6} (8.88 \cdot 10^{-7})$	115.92 (3649)	<0.0001
T	$5.24 \cdot 10^{-4} (1.32 \cdot 10^{-4})$	15.75 (37)	0.0003
Y_r	$-6.08 \cdot 10^{-3} (1.79 \cdot 10^{-3})$	11.47 (37)	0.0017
Y_r^2	$1.52 \cdot 10^{-6} (4.53 \cdot 10^{-7})$	11.23 (37)	0.0019
xY_r	$7.21 \cdot 10^{-7} (1.49 \cdot 10^{-7})$	23.42 (3649)	<0.0001
xT	$-1.12 \cdot 10^{-5} (2.35 \cdot 10^{-6})$	22.50 (3649)	<0.0001

negative month effect (likely due to month not being included as an increasing variable within sampling year), whereas the month effect found in our model was positive (see Fig. S2.2 for the observed mean across year and month). Second, Edeline *et al.* (2007) concluded that egg weight had been maintained over time, as the year effect was not significant in their model. Our model suggested a non-linear year effect with an initial decrease and then an increase, and also included an interaction of year with length (Fig. S2.2). Third, Edeline *et al.* (2007) included an age effect and only a linear length effect, whereas we included a quadratic effect of length and no age effect, leading to practically the same predictions of egg weight as a function of length. We did not include age because it is highly correlated with length.

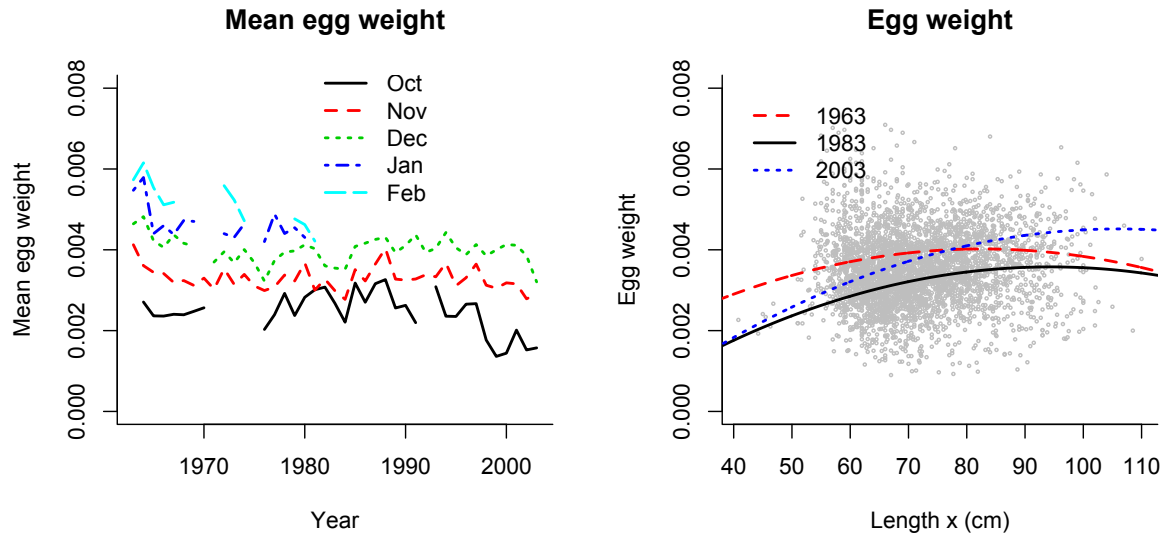


Figure S2.2: Left: Observed trends in the mean egg weight (for all individuals) across capture year and month. Right panel: Predicted effect of length on fecundity in the final model, for three different years.

S2-3. Offspring length

The distribution of next year's offspring lengths (measured at age 1), $f(y'; T)$, was assumed to be lognormal with mean $\mu_1(T)$ and constant variance σ_1^2 . As we did not have data on how offspring length depends on maternal traits, we also assumed no heritability (i.e. no effect of maternal length at age 1 on offspring length at age 1) in the model used in the main text. In appendix C5 we present some results for a model assuming a correlation of 0.3 between maternal and offspring length at age 1.

All candidate models considered for offspring length included year as a random effect. The global model for the fixed effects was given by

$$\mu_1(T) \sim Y_r + T + Y_r T,$$

where Y_r is year and T is temperature. The highest ranked model included all effects except for the interaction, and was selected for the IPM (table S2.5). Table S2.6 shows the resulting fixed effects in the selected model, after refitting using restricted maximum likelihood. In the offspring length model used in the main analysis year was fixed equal to its mean (year 1965).

Table S2.5: Model selection table for fixed effects in the model for offspring length, showing the highest ranked candidate models based on AICc. Covariates considered were temperature T and year Y_r . All candidate models included year as a random effect, and were estimated using maximum likelihood.

Model	T	Y_r	TY_r	df	logLik	AICc	Δ AICc	weight
1	*	*		5	-21203	42415	0.00	0.638
2	*	*	*	6	-21202	42417	1.83	0.256
3		*		4	-21205	42419	3.67	0.102
4	*			4	-21208	42425	9.83	0.005
	5			3	-21214	42433	17.85	0.000

Table S2.6: Effects and statistical significance (marginal tests) for the model for mean length at age 1 $\mu_1(T)$ used in the IPM (model 1 from table S2.5, re-fitted using restricted maximum likelihood). The variance of the random year effect was 1.069, and the residual variance was 12.30. In the main analysis year was kept constant at 1965.

Fixed effect	Estimate (SE)	F-value (denDF)	p-value
(Int)	$-6.34 \cdot 10 (2.21 \cdot 10)$	8.21 (7857)	0.0550
T	$6.53 \cdot 10^{-1} (2.74 \cdot 10^{-1})$	5.67 (47)	0.0213
Y_r	$4.06 \cdot 10^{-2} (1.16 \cdot 10^{-2})$	12.28 (47)	0.0010

Figure S2.3 shows the observed (i.e. including backcalculated values) mean

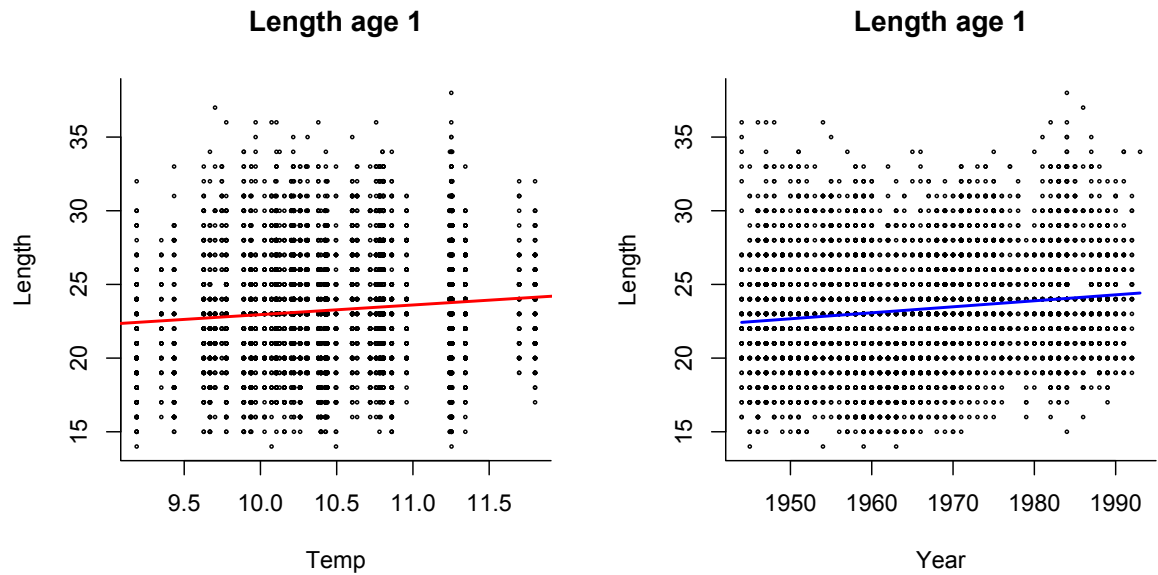


Figure S2.3: Length at age 1 as a function of temperature (left) and as a function of year (right), as predicted from the selected model.

length at age 1 (for all individuals) across temperature and years, together with predictions from the model. Both the temperature and the year effect are positive, as in the model of Vindenes *et al.* (2014).

S2-4. Somatic growth

The distribution of next year's length $g(x'; x, y, T)$ was assumed to be a truncated lognormal distribution (truncated to not allow shrinking), with mean $\mu_G(x, y, T)$ and variance $\sigma_G^2(x)$. The mean and variance functions were estimated from back-calculated length data for females using a mixed effects model with next year's length as the response variable, and where the covariates considered were current length, offspring length at age 1, year, and temperature. The time series (1944-1995) was cut off at 1992, because in the final years the back-calculated length estimates are uncertain due to few individuals in the data (pike are not susceptible to the sampling before an age of about 3 years so that the length estimates of especially the youngest age classes are uncertain towards the end of the time series). The resulting time series used for the growth calculation was from 1944-1992 (7907 individuals). Without cutting off the time series, there is an apparent final increase in mean length at age for age classes 1-3 in the final years of the time series, however these points are based on just 1 fish that was caught at age 3 in 1995 (and happened to be a large one).

All candidate models considered included year as a random effect and an exponential variance function with current length as a covariate, which defines $\sigma_G^2(x)$. Because growth rate is not a linear function of length and because there are few data points for large compared to smaller individuals, we included several higher order effects of length (up to order 4) in the candidate models. This allows more flexibility to correctly estimate the slower growth rate of the largest individuals, which might otherwise be too much influenced by the data points corresponding to smaller individuals. The global model for the fixed effects was given by

$$x' \sim x + y + Y_r + T + x^2 + x^3 + x^4 + T^2 + xT + xy + x^2y,$$

where x is current length, y is length at age 1, Y_r is year and T is temperature. The model selection table (table S2.7) shows that the highest ranked model excluded only the second order temperature effect. The second highest ranked model also excluded the interaction between x^2 and y , and had a $\Delta \text{AICc} = 0.89$ in comparison to the highest ranked. This model was chosen for the IPM, and table S2.8 shows the resulting fixed effects after refitting using restricted maximum likelihood. The model for variance in growth was given by $\sigma_G^2(x) = 11.2e^{-0.0081x}$. In the main analysis year was kept constant at a value equal to the mean (1966).

Because of size-specific gill net selection, few pike are caught until they reach a length of ~ 55 cm, around 3 years of age (Frost & Kipling, 1967). Given that survival generally increases with body length, the somatic growth rate estimated from the back-calculated length data will therefore be biased upward for lengths corresponding to the youngest ages, since the growth model does not account for length-specific survival differences. We assessed the size of the bias by comparing the predicted length distribution from the IPM with the length distribution in the data, and it was not very large (a maximum of around 3 cm at age 2). We did not correct for this bias in the current study, as this would not change any qualitative conclusions.

Table S2.7: Model selection table for fixed effects in the growth model (determining mean length $\mu_G(x, y, T)$), showing the highest ranked candidate models based on AICc. Covariates considered were current length x , length at age 1 y , temperature T , and year Y_r . All models included year as a random effect, and an exponential variance function with length as a covariate. Candidate models were estimated using maximum likelihood.

Model	y	x	x^2	x^3	x^4	T	T^2	Y_r	xy	x^2y	xT	df	logLik	AICc	ΔAICc	weight
1	*	*	*	*	*	*	*	*	*	*	*	14	-58916	117859.9	0.00	0.430
2	*	*	*	*	*	*	*	*	*	*	*	13	-58917	117860.7	0.89	0.276
3	*	*	*	*	*	*	*	*	*	*	*	15	-58916	117861.6	1.75	0.179
4	*	*	*	*	*	*	*	*	*	*	*	14	-58917	117862.5	2.63	0.115
5	*	*	*	*	*	*	*	*	*	*	*	13	-58930	117886.5	26.64	0.000

Table S2.8: Effects and statistical significance (marginal tests) for the mean of the final somatic growth model $\mu_G(x, y, T)$ used in the IPM (model 2 from table S2.7, re-fitted using restricted maximum likelihood). The estimated variance of the random year effects was 0.559, the residual variance was 3.352, and the estimated parameter for the exponential variance function was -0.0081. In the main analysis year was kept constant equal to the mean (1966).

Fixed effect	Estimate (SE)	F-value (denDF)	p-value
(Int)	-1.01 · 10 ² (2.00 · 10)	569399 (25877)	<0.0001
x	2.79 (4.36 · 10 ⁻²)	968524 (25877)	<0.0001
x^2	-4.54 · 10 ⁻² (1.24 · 10 ⁻³)	584 (25877)	<0.0001
x^3	4.59 · 10 ⁻⁴ (1.51 · 10 ⁻⁵)	4347 (25877)	<0.0001
x^4	-1.59 · 10 ⁻⁶ (6.49 · 10 ⁻⁸)	800 (25877)	<0.0001
y	3.71 · 10 ⁻¹ (1.21 · 10 ⁻²)	2537 (25877)	<0.0001
Y_r	4.078 · 10 ⁻² (6.25 · 10 ⁻³)	37 (45)	<0.0001
T	1.32 (1.58 · 10 ⁻¹)	149 (45)	<0.0001
xT	-1.42 · 10 ⁻² (1.26 · 10 ⁻³)	163 (25877)	<0.0001
xy	-4.10 · 10 ⁻³ (2.21 · 10 ⁻⁴)	344 (25877)	<0.0001

Figure S2.4 shows the observed mean length at age together with predictions from the model for three values of offspring length y . The model predictions assuming $y = 23\text{cm}$ (\sim mean offspring length) closely follows the observed mean, however for very old ages (>15) the predictions are more uncertain due to few data. The model indicates that pike that are large as offspring tend to grow faster and stay larger at a given age except for the oldest ages. There was also a positive but weak linear year effect on somatic growth (Fig. S2.4).

The predicted somatic growth rates of this model are largely the same as in growth model of Vindenes & Langangen (2015), except for the largest lengths. Vindenes & Langangen (2015) only included effects of length up to the second order, whereas here a third and fourth order effect were also included, which more accurately captures the growth rate of the largest individuals. For small and intermediate pike the model predictions are very similar to the model of Vindenes & Langangen (2015), but for the largest individuals the current model predicts

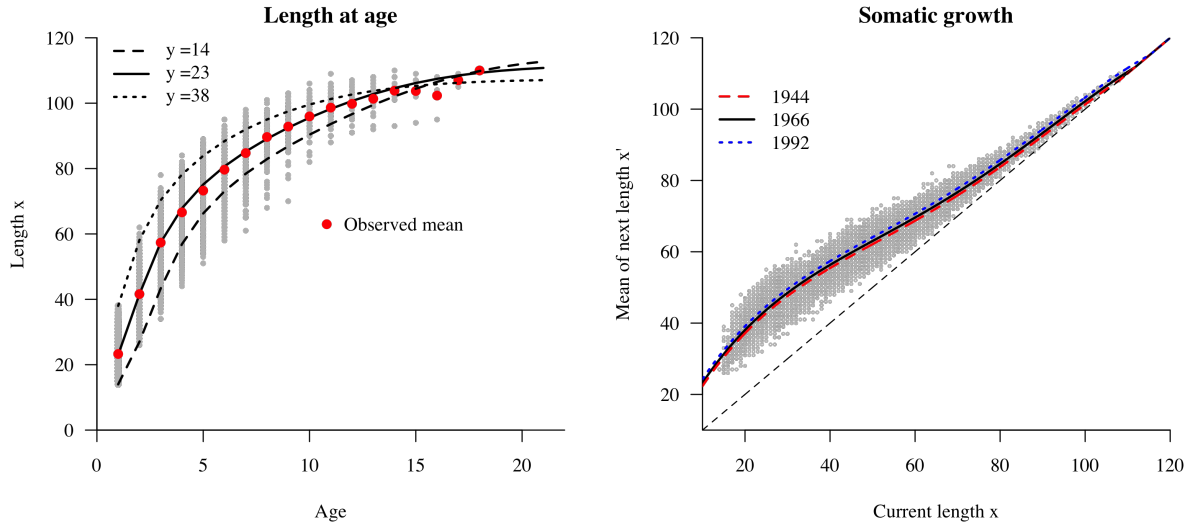


Figure S2.4: Left. Length at age predicted from the fitted model, for three different lengths at age 1 (y), together with the observed (including back-calculated) mean length at age (red dots, grey dots are data points). Right: Mean length next year ($\mu_G(x, y, T)$) as a function of current length x , for three different years.

a higher growth rate. Since only a few individuals in the population will reach the largest lengths, the IPM results are not much affected by underestimating the growth at large lengths. However, we still include the higher order effects here in order to get a more correct growth model also for these individuals.

The current growth model suggests that a slow-growing cohort may arise if it experiences low temperature during the first year(s). The slowest growing cohorts observed in the data were born in the early 1960s (1961-1965). Edeline *et al.* (2007) suggested that their slow growth represented a rapid evolutionary response to high fishing pressure in those years (1962-1965, with a peak in fishing pressure in 1963; Fig. 1 of Edeline *et al.*, 2007). However, these cohorts also experienced multiple cold years over the beginning of their life (Fig. S1.1), so that plastic responses of growth to temperature represent a likely alternative explanation for the slow growth. In their growth model, Edeline *et al.* (2007) included effects of

current temperature and year, but not lasting effects of temperature during the first year of life. Also, the peak in fishing pressure occurred in 1962-1963, but the first slow growing cohort appeared in 1961. In 1961 the average temperature was not particularly low, however the subsequent cold years (1962-1965; Fig. S1.1) would still lead to a slow growing cohort according to our model.

Figure S2.5 shows the observed mean length in different age classes as a function of temperature during the first year of life, reflecting the positive relationship except for the oldest ages, although there is also much variation. While our growth model highlights the importance of temperature, growth is also affected by many other factors not explicitly considered here, in particular food availability (Kipling, 1983). Here, such factors are included in the residual variance, and systematic temporal changes are captured by the fixed year effect. Figure S2.6 shows the mean length at age against temperature of the current year, also suggesting positive effects for all ages except the oldest (where the effect is weaker).

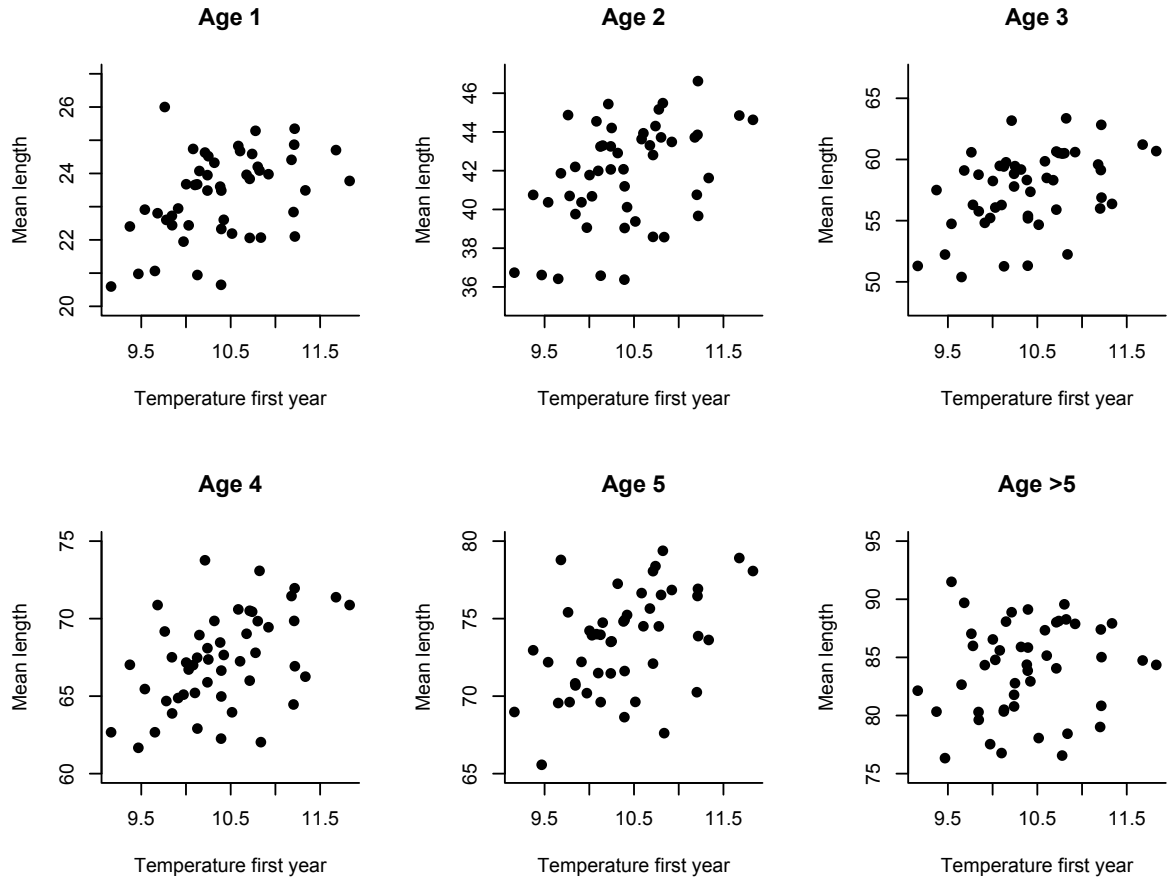


Figure S2.5: Mean length at age plotted against temperature experienced during the first year of the cohort, showing a positive relationship as predicted by the growth model.

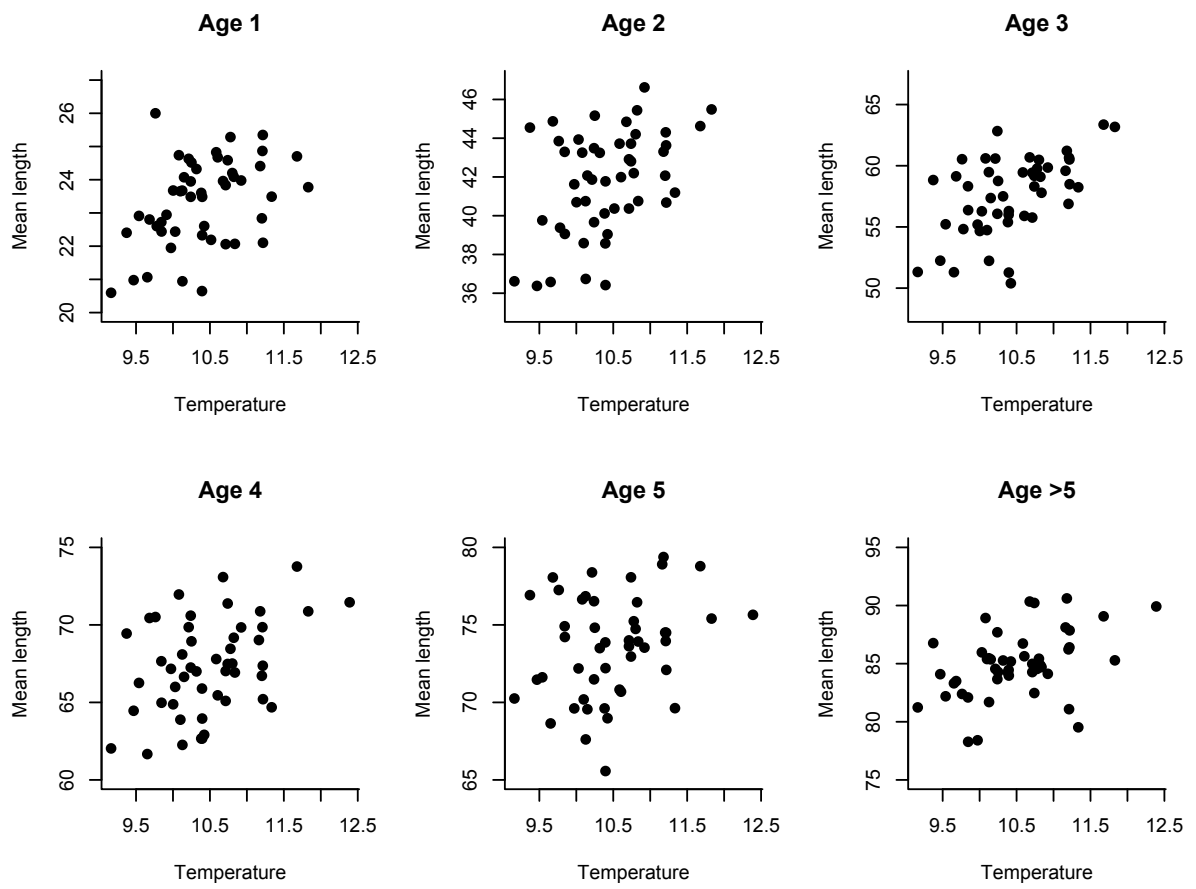


Figure S2.6: Mean length at age plotted against temperature of the current year, showing a positive relationship as predicted by the growth model.

S2-5. Survival probability

The survival probability $s(x, y, T)$ was estimated using the same method as in Vindenes *et al.* (2014), based on an iterative Monte Carlo procedure incorporating the growth model. Because the growth model used here is different from that study we updated the survival model accordingly. The resulting survival probability function was very similar to that of Vindenes *et al.* (2014), indicating that the changes to the growth model did not have a large impact on the survival probability estimate. The effect of length at age 1 y could not be estimated from data, however Vindenes & Langangen (2015) noticed that the age at capture in the winter sampling tended to decline with length at age 1, suggesting a possible negative effect of y on survival. Therefore, we included a negative effect of y in the final survival model (after estimation), but note that the sensitivities to other variables in the IPM are largely unaffected by whether or not this effect is included.

The survival data contain survival and length information on individuals based on capture-mark-recapture (Carlson *et al.*, 2007). The iterative resampling procedure of Vindenes *et al.* (2014) used the capture probabilities estimated by Carlson *et al.* (2007) to calculate the cumulative probability that an individual is still alive but not recaptured. This probability approaches zero after a few years (Windermere is a closed system). In each iteration a model for fixed effects was fitted (using a mixed model on logit scale with year as a random effect), given by

$$\text{logit}(s(x, T)) \sim x + Y_r + T + x^2 + xT,$$

where x is current length, Y_r is year, and T is temperature. After a few iterations the estimated parameters of the survival function approached a stationary distribution. We discarded the results from the first 100 iterations (much more than

required for convergence), and then stored the results from the following 1000 iterations. The effects used in the final survival model are the mean effects from these iterations, shown in table S2.9. The variance of the averaged random year effects was 0.0095. Figure S2.7 shows the histogram for each of the survival effects from the 1000 iterations, while figure S2.8 shows the realized effects plotted against each other, indicating the correlation structure. While the histogram of the main effect of temperature overlaps zero, this effect is strongly correlated with the interaction effect (fig. S2.8) and together they consistently show a negative impact of temperature at intermediate/large lengths. In figure S2.9 the survival probability function (assuming constant survival at large lengths) is shown for three values of the temperature effect, with corresponding values for the other effects based on the relationships shown in figure S2.8 (estimated using linear models). In all cases the survival model remains qualitatively similar with an overall negative effect of temperature for intermediate to large lengths (some potential underlying mechanisms of this effect are discussed by Vindenes *et al.*, 2014).

Table S2.9: Effects in the survival probability model $\text{logit}(s(x, y, T))$ used in the IPM, calculated from the mean and standard deviation based on 1000 sample estimates. Covariates considered were current length x , temperature T , and year Y_r . In addition to these effects, a negative effect of length at age 1 y was included in the final model (not estimated from data).

Fixed effect	Estimate (SE)
(Int)	$7.33 \cdot 10^{-1}$ (3.58)
x	$4.89 \cdot 10^{-1}$ ($3.89 \cdot 10^{-2}$)
x^2	$-3.74 \cdot 10^{-3}$ ($1.27 \cdot 10^{-4}$)
T	$1.93 \cdot 10^{-1}$ ($1.84 \cdot 10^{-1}$)
Y_r	$-4.37 \cdot 10^{-2}$ ($1.31 \cdot 10^{-3}$)
xT	$-6.84 \cdot 10^{-3}$ ($3.48 \cdot 10^{-3}$)
y	$-5 \cdot 10^{-2}$

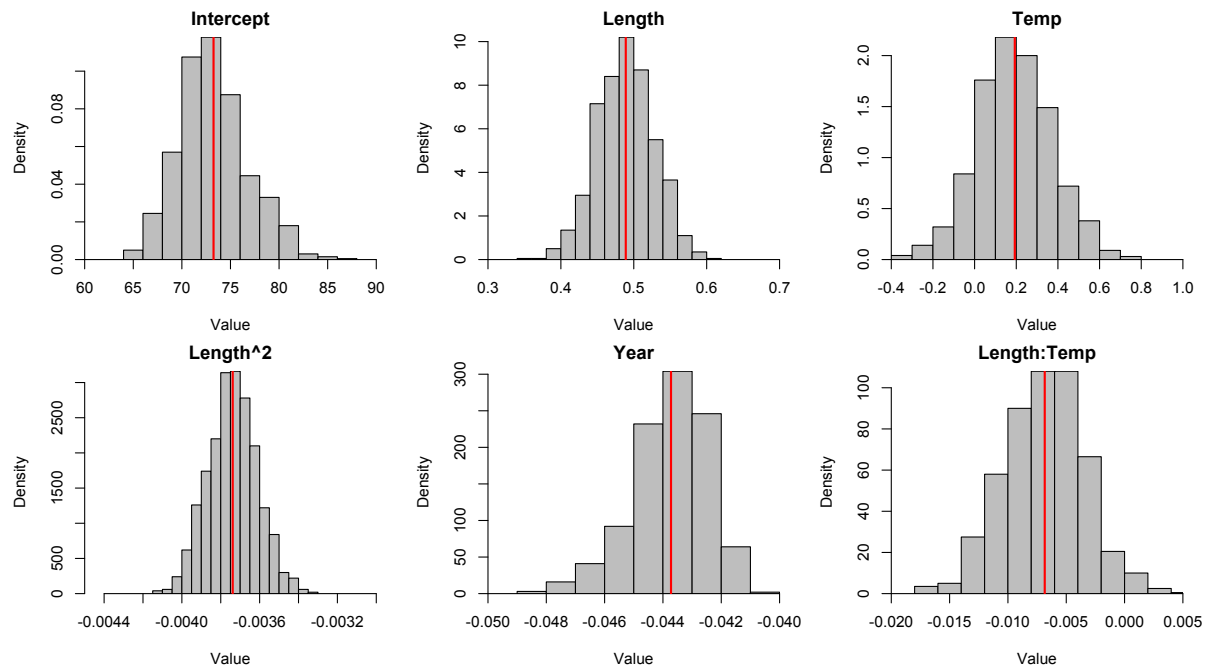


Figure S2.7: Histogram of effects in the survival function from 1000 iterations (after discarding the results for the first 100 iterations), using the method of Vindenes *et al.* (2014) with an updated growth function. Note that the temperature and length effects are positively correlated (Fig. S2.8) and that the overall temperature effect is always negative for intermediate/large lengths (Fig. S2.9).

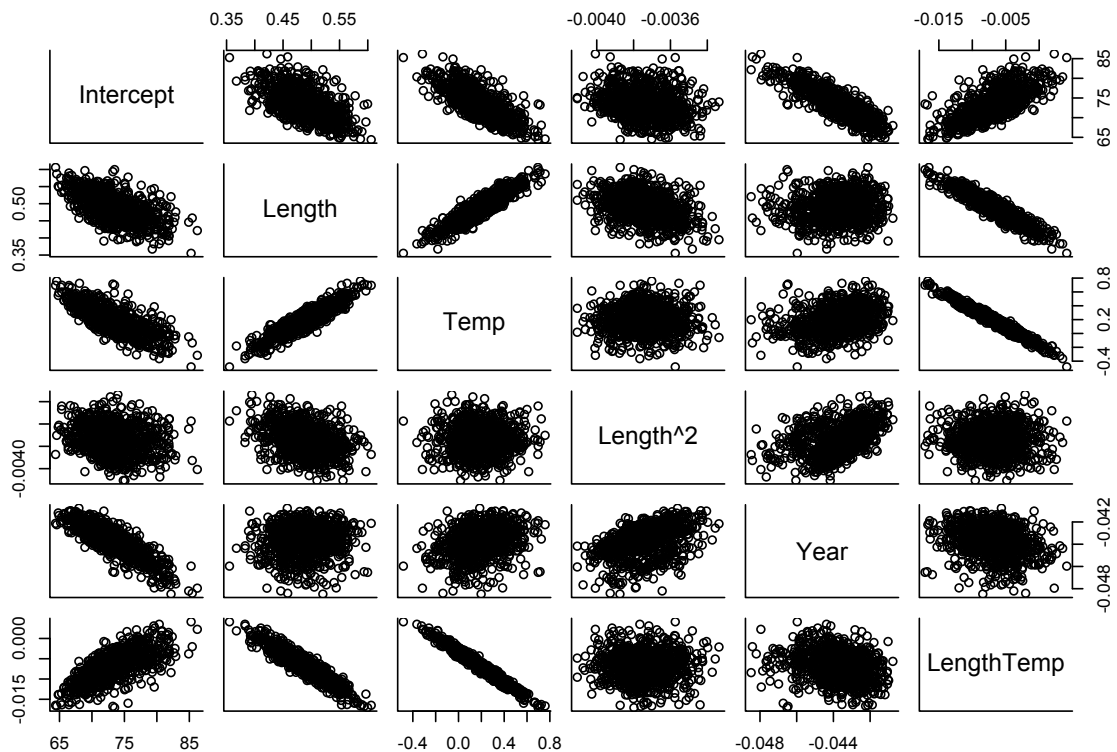


Figure S2.8: Relationships between the estimated effects in the survival model from 1000 iterations of the resampling model.

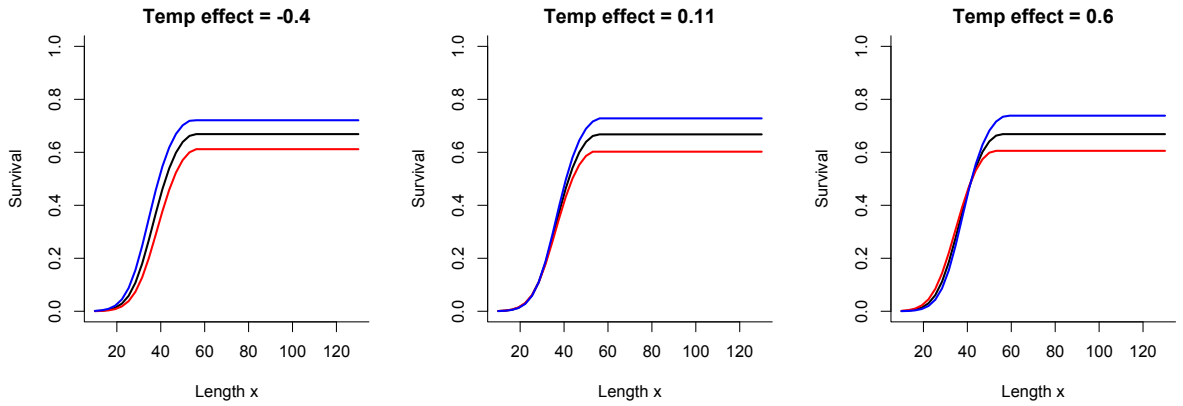


Figure S2.9: The overall effect of temperature on survival for different values of the main temperature effect, adjusting the intercept, interaction effect and length effect according to the relationships shown in figure S2.8 (estimated from a linear model of each effect against the temperature effect). Blue lines correspond to 9 °C, black lines to 10.5 °C, and red lines to 12 °C.

Appendix S3: Methods and additional results to sensitivity and elasticity analyses

In this appendix we show the detailed expressions for the decomposition of the elasticities presented in the main text, as well as some supporting results from additional analyses. Corresponding sensitivities are also shown. The results presented here include elasticities evaluated at different temperatures, results from a model including heritability of offspring length, and results from a model assuming a stronger maternal effect of length on egg weight than indicated by the data.

S3-1. Sensitivity and elasticity to the projection kernel

The sensitivity and elasticity of λ to the projection kernel are calculated in the same way as for a matrix model (Caswell, 2001). The sensitivity kernel is given by

$v(x', y')u(x, y)$ (Ellner & Rees, 2006), where $v(x, y)$ and $u(x, y)$ are scaled so that $\int \int u(x, y)dx dy = 1$ and $\int \int u(x, y)v(x, y)dx dy = 1$. This shows the sensitivity of λ to an infinitesimal additive perturbation of the projection kernel, including areas where perturbations may not be biologically realistic. The elasticity kernel shows the predicted effect on λ of proportional perturbations of the projection kernel, and is given by $v(x', y')u(x, y)K(x', y'; x, y)/\lambda$. The elasticity and sensitivity kernels can look very different for life histories such as those of highly fecund fishes, where values in the projection kernel can differ by several orders of magnitude (Caswell, 2001). Note that the elasticity kernel integrates to 1, but in general this is not the case for elasticities to underlying variables (Caswell, 2001).

For IPMs the sensitivity kernel can be difficult to interpret biologically as the projection kernel typically have many areas with values that are close to (but not quite) zero. For matrix models it is common to show sensitivities only for stages of the projection matrix where perturbations are biologically realistic, usually corresponding to the non-zero entries (Caswell, 2001). For IPMs having continuous state variables, however, it can be difficult to define exactly where the areas of such unrealistic changes would begin. The interpretation of the elasticity kernel is not limited in the same way, as areas of the projection kernel that are close to zero will also generally have a low elasticity (since the projection kernel enters as a factor in the elasticity).

S3-2. Sensitivity and elasticity to underlying parameters

Using the same approach as that of Vindenes *et al.* (2014) based on applying the chain rule, the sensitivity of λ with respect to some underlying variable θ (where θ could represent x , or y , or T in our model) can be decomposed into contributions across length x ,

$$\begin{aligned}\frac{d\lambda}{d\theta}(x) &= \int \int \int \frac{d\lambda}{dK(x', y'; x, y, \theta)} \frac{dK(x', y'; x, y, \theta)}{d\theta} dy dx' dy' \\ &= \int \int \int v(x', y') u(x, y) \frac{dK(x', y'; x, y, \theta)}{d\theta} dy dx' dy',\end{aligned}$$

where all integrals are over the entire range of state variables (x and y). It is also possible to do a similar decomposition across offspring length y , but for this study the most relevant decomposition is across length x . The sensitivity of the projection kernel with respect to θ can be further decomposed into contributions from each vital rate, as shown below for each specific case of sensitivity with respect to x , y , or T .

Notation alert: We use the notation $\frac{d\lambda}{d\theta}(x)$ when the sensitivity is evaluated at a specific value of x (including when the sensitivity is to x itself). The total sensitivity of λ to θ is given by $\frac{d\lambda}{d\theta} = \int \frac{d\lambda}{d\theta}(x) dx$.

The corresponding elasticity to θ (i.e. the sensitivity of $\ln \lambda$ to $\ln \theta$) at a given value of x is given by

$$\frac{\theta}{\lambda} \frac{d\lambda}{d\theta}(x) = \int \int \int \frac{\theta}{\lambda} v(x', y') u(x, y) \frac{dK(x', y'; x, y, \theta)}{d\theta} dy dx' dy'.$$

Thus, unless θ represents current length x , the elasticity contributions across x are simply a rescaling of the sensitivity contributions. For length x , the relative elasticity contributions will be different from the sensitivity contributions across x , with higher relative contributions from large lengths. The total elasticity is given by $\int \frac{\theta}{\lambda} \frac{d\lambda}{d\theta}(x) dx$. In the following, we show the detailed expression for each elasticity

(and corresponding sensitivity) decomposition considered in the main text.

Sensitivity and elasticity to current female length x

With respect to current length x , the sensitivity contribution measured at a given value of x is given by (to simplify notation we omit temperature T from the expression here)

$$\begin{aligned}\frac{d\lambda}{dx}(x) &= \int \int \int \frac{d\lambda}{dK(x', y'; x, y)} \frac{dK(x', y'; x, y)}{dx} dy dx' dy' \\ &= \int \int \int v(x', y') u(x, y) \left[\frac{ds(x, y)}{dx} g(x'; x, y) \delta(y' - y) + \frac{dg(x'; x, y)}{dx} s(x, y) \delta(y' - y) \right. \\ &\quad + 0.5 \frac{dm(x)}{dx} s_O(w(x)) p_m(x) f(y') \delta(y' - x') + 0.5 \frac{ds_O(w(x))}{dx} m(x) p_m(x) f(y') \delta(y' - x') \\ &\quad \left. + 0.5 \frac{dp_m(x)}{dx} s_O(w(x)) m(x) f(y') \delta(y' - x') \right] dy dx' dy'.\end{aligned}$$

The corresponding elasticity is given by $\frac{x}{\lambda} \frac{d\lambda}{dx}(x)$. The last expression in the above equation for $\frac{d\lambda}{dx}(x)$ contains five terms that each correspond to the contributions from one vital rate (in this case from survival, growth, fecundity, offspring survival, and probability of maturity). The sensitivity contributions from vital rates where x has no effect (e.g. offspring length) are naturally zero. The maternal effect of length on egg weight is included within the sensitivity contribution from offspring survival,

$$\frac{ds_O(w(x))}{dx} = \frac{ds_O(w(x))}{dw} \frac{dw(x)}{dx}.$$

Sensitivity and elasticity to female offspring length y

With respect to offspring length y , the sensitivity contribution at a given length x is given by (again, temperature T is omitted to simplify the expression)

$$\begin{aligned}\frac{d\lambda}{dy}(x) &= \int \int \int \frac{d\lambda}{dK(x', y'; x, y)} \frac{dK(x', y'; x, y)}{dy} dx' dy dy' \\ &= \int \int \int v(x', y') u(x, y) \left[\frac{ds(x, y)}{dy} g(x'; x, y) \delta(y' - y) \right. \\ &\quad \left. + \frac{dg(x'; x, y)}{dy} s(x, y) \delta(y' - y) \right] dy dx' dy'.\end{aligned}$$

The corresponding elasticity is given by $\frac{y}{\lambda} \frac{d\lambda}{dy}(x)$. Since female offspring length affects only two vital rates in the model (survival and growth), there are only two vital rate terms in the above decomposition.

Sensitivity and elasticity to temperature T

The sensitivity to temperature T at a given value of female length x is given by (assuming $T^* = T$)

$$\begin{aligned}\frac{d\lambda}{dT}(x) &= \int \int \int \frac{d\lambda}{dK(x', y'; x, y, T)} \frac{dK(x', y'; x, y, T)}{dT} dx' dy dy' \\ &= \int \int \int v(x', y') u(x, y) \left[\frac{ds(x, y, T)}{dT} g(x'; x, y, T) \delta(y' - y) \right. \\ &\quad \left. + \frac{dg(x'; x, y, T)}{dT} s(x, y, T) \delta(y' - y) \right. \\ &\quad \left. + 0.5 \frac{ds_O(w(x, T), T)}{dT} m(x) p_m(x) f(y'; T) \delta(y' - x') \right. \\ &\quad \left. + 0.5 \frac{df(y'; T)}{dT} m(x) p_m(x) s_O(w(x, T), T) \delta(y' - x') \right] dx' dy dy'.\end{aligned}$$

The corresponding elasticity is given by $\frac{T}{\lambda} \frac{d\lambda}{dT}(x)$. In this case there are four terms each corresponding to the sensitivity contribution of a vital rate (survival, growth, offspring survival, and offspring length). In addition, temperature affects offspring survival function both directly (during the spawning year) and indirectly via egg weight. To separate these two, the offspring survival component can be decomposed further using the chain rule:

$$\frac{ds_O(w(x, T), T)}{dT} = \frac{ds_O(w, T)}{dw} \frac{dw}{dT} + \frac{ds_O(w, T)}{dT}.$$

The first term represents the sensitivity contribution through temperature effects on egg weight (estimated by the data), whereas the second term represents the direct contribution through offspring survival (value unknown in our model).

S3-3. Elasticities evaluated at different temperatures

For the results presented in the main text elasticities were evaluated at the mean temperature ($T^* = T$) of 10.5°C. Here, we explore how the results change if the elasticities are calculated at different temperatures (9°C and 12°C, respectively, representing cold and warm conditions, see temperature time series in fig. S1.1). Figure S3.1 shows how λ changes with temperature depending on the scenario for offspring survival. The strongest non-linearity occurs for scenario 1 (interaction) and 3 (temperature), whereas models for scenarios 2 and 4 show much more linear relationships. Figure S3.2 shows the elasticity to temperature decomposed into contributions from each vital rate across x , evaluated at 9°C, 10.5°C, and 12°C (for corresponding sensitivities, see fig. S3.3). Overall, within each scenario the ranks of most elasticities remain the same (although some are shifting), as do the patterns over length. For scenario 1 assuming a negative correlation between

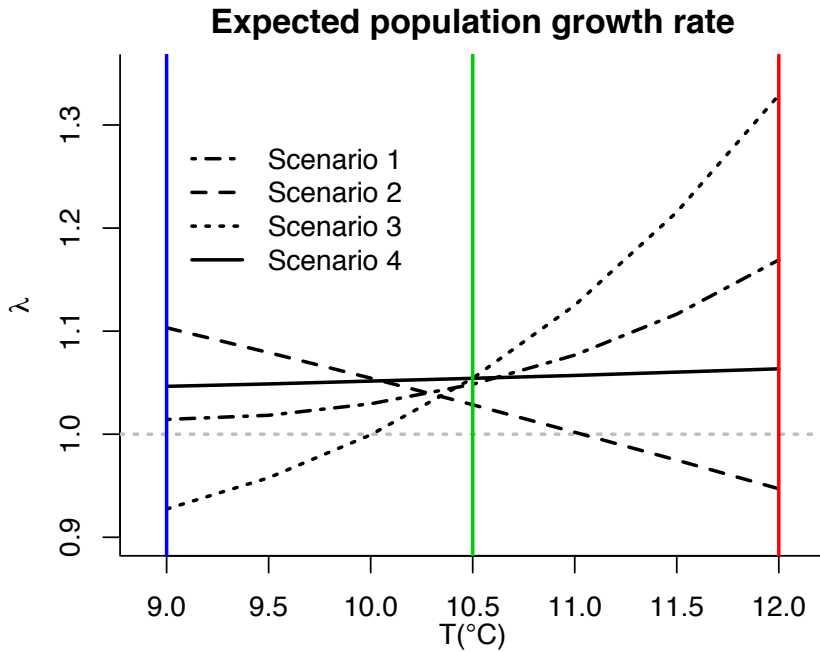


Figure S3.1: Population growth rate λ as a function of temperature, for the four different scenarios.

temperature and egg weight on offspring survival, the elasticity to temperature through egg weight also changes sign from negative at 9°C and 10.5°C to positive at 12 °C, reflecting the advantage of producing smaller eggs in warm conditions.

The decomposition of the elasticity to female current length also changed only slightly when evaluated at different temperatures (fig. S3.4; for corresponding sensitivities see fig. S3.5). Note that for scenario 2 (assuming a strong positive effect of egg weight on offspring survival), the elasticity contribution via egg weight declines with temperature and is largest at $T = 9^{\circ}\text{C}$, but still quite small compared to the other sensitivities. Cold conditions correspond to the steepest slope of the relationship between female length and egg weight (Fig. 2A in the main text). In addition, individuals grow at a slower rate, so that a larger proportion of reproductive females are within the size range corresponding to the steepest slope. The

temperature effect on egg weight is also negative, so that larger eggs are produced under cold conditions, increasing the overall impact of egg weight (and also the elasticity to female length on egg weight) on population dynamics.

The decomposition of the elasticity to female offspring length remains largely the same when evaluated at different temperatures (fig. S3.6; for corresponding sensitivities see fig. S3.7), with the negative impact through survival being stronger than the positive effect on growth under all scenarios and temperatures.

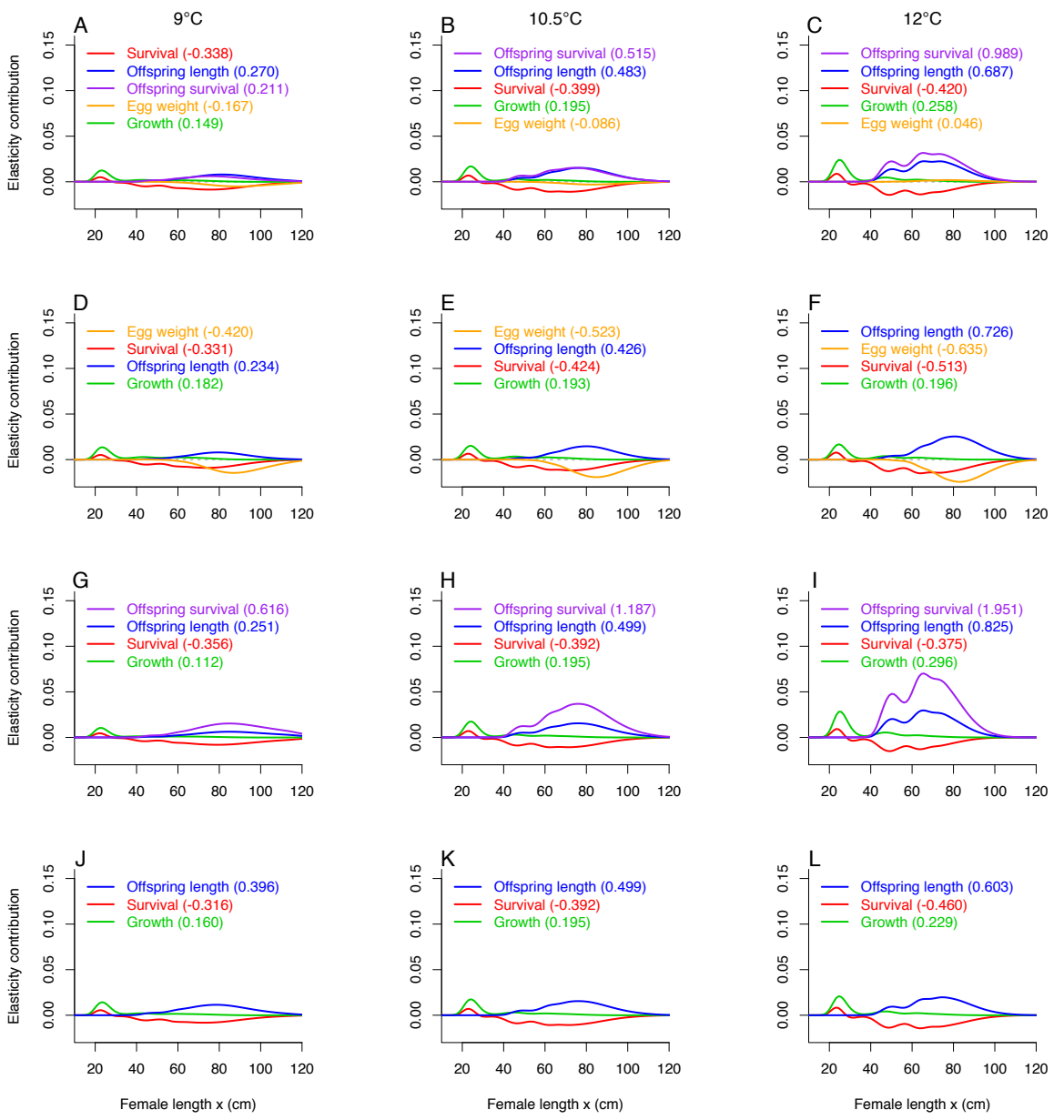


Figure S3.2: Elasticity of λ with respect to temperature T , decomposed into contributions from different vital rates across length x . The elasticity is evaluated for three different temperatures (Panels A, D, G, J: 9°C; panels B, E, H, K: 10.5°C; and panels C, D, I, L: 12°C), and for four different offspring survival scenarios (panels A, B, C: Scenario 1 Interaction; B, C, D: Scenario 2 Size; G, H, I: Scenario 3 Temperature; and J, K, L: Scenario 4 None). The total elasticity for each vital rate (integrated over x) is shown in the legends, listed by magnitude of absolute value.

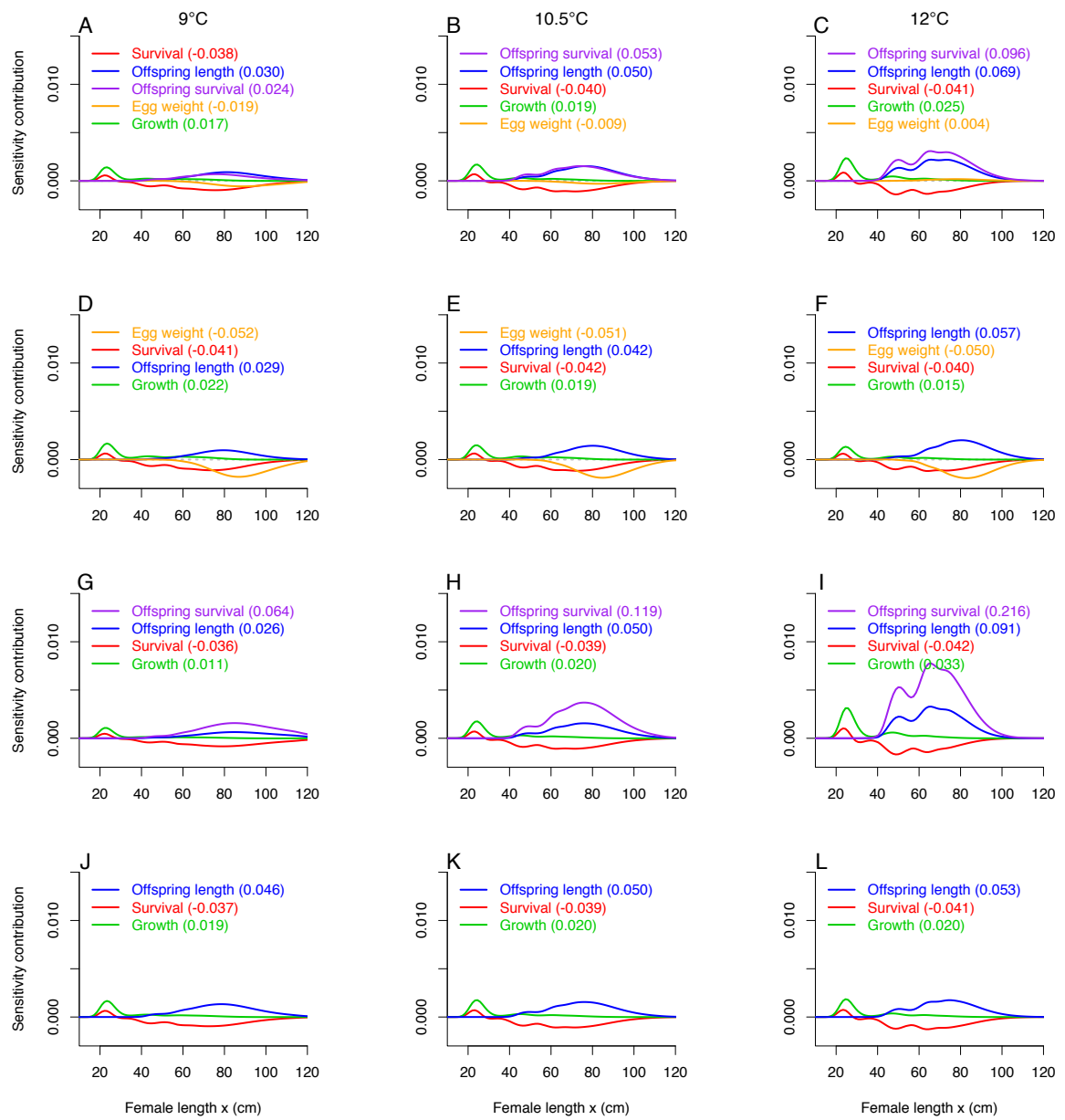


Figure S3.3: Sensitivity results corresponding to the elasticity results in figure S3.2. Sensitivity of λ with respect to temperature T , decomposed into contributions from different vital rates across length x . The sensitivity is evaluated for three different temperatures (Panels A, D, G, J: 9°C; panels B, E, H, K: 10.5°C; and panels C, D, I, L: 12°C), and for four different offspring survival scenarios (panels A, B, C: Scenario 1 Interaction; B, C, D: Scenario 2 Size; G, H, I: Scenario 3 Temperature; and J, K, L: Scenario 4 None). The total sensitivity for each vital rate (integrated over x) is shown in the legends, listed by magnitude of absolute value.

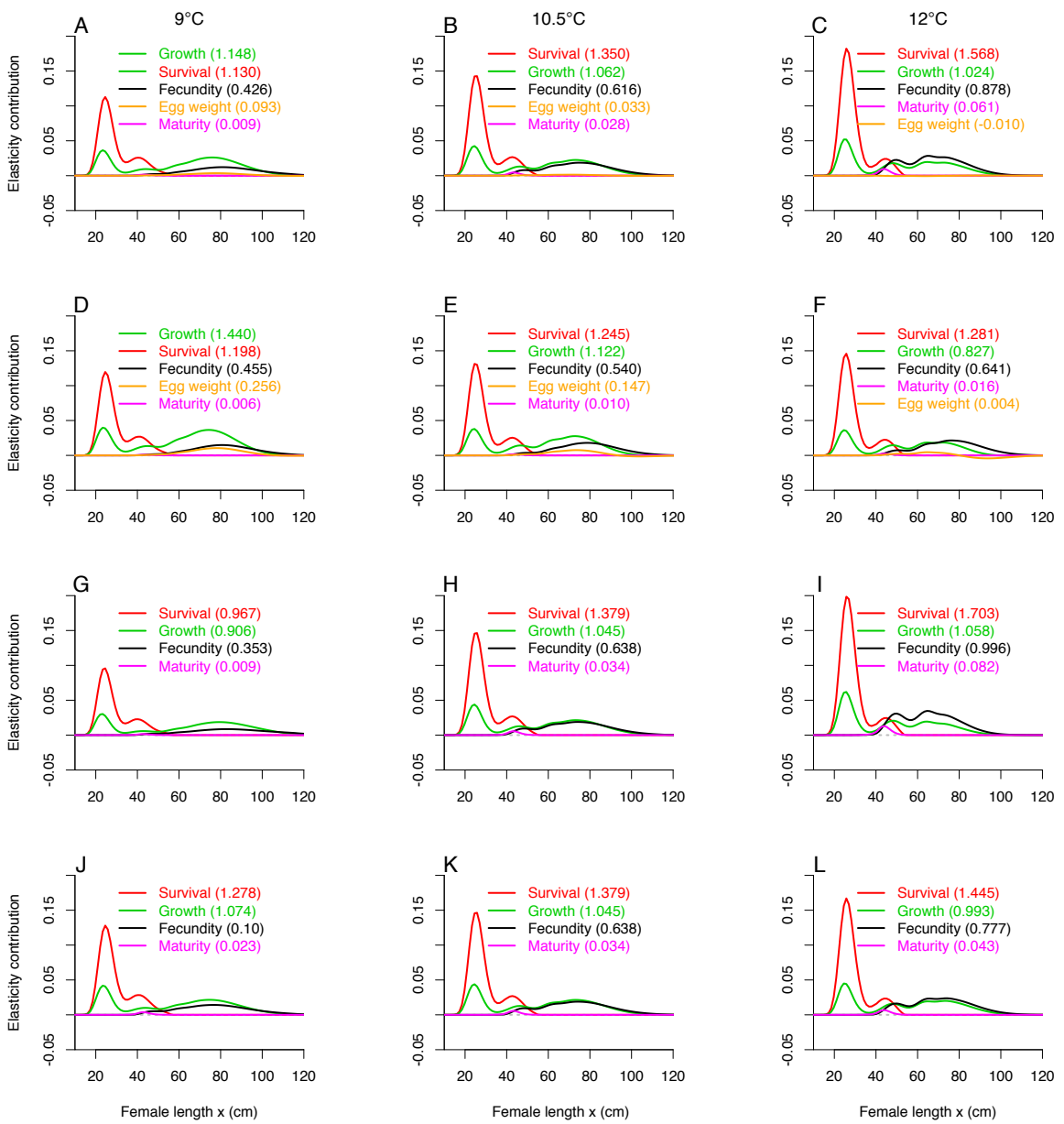


Figure S3.4: Elasticity of λ with respect to female current length x , decomposed into contributions from different vital rates across length x . The elasticity is evaluated for three different temperatures (Panels A, D, G, J: 9°C; panels B, E, H, K: 10.5°C; and panels C, D, I, L: 12°C), and for four different offspring survival scenarios (panels A, B, C: Scenario 1 Interaction; B, C, D: Scenario 2 Size; G, H, I: Scenario 3 Temperature; and J, K, L: Scenario 4 None). The total elasticity for each vital rate (integrated over x) is shown in the legends, listed by magnitude of absolute value.

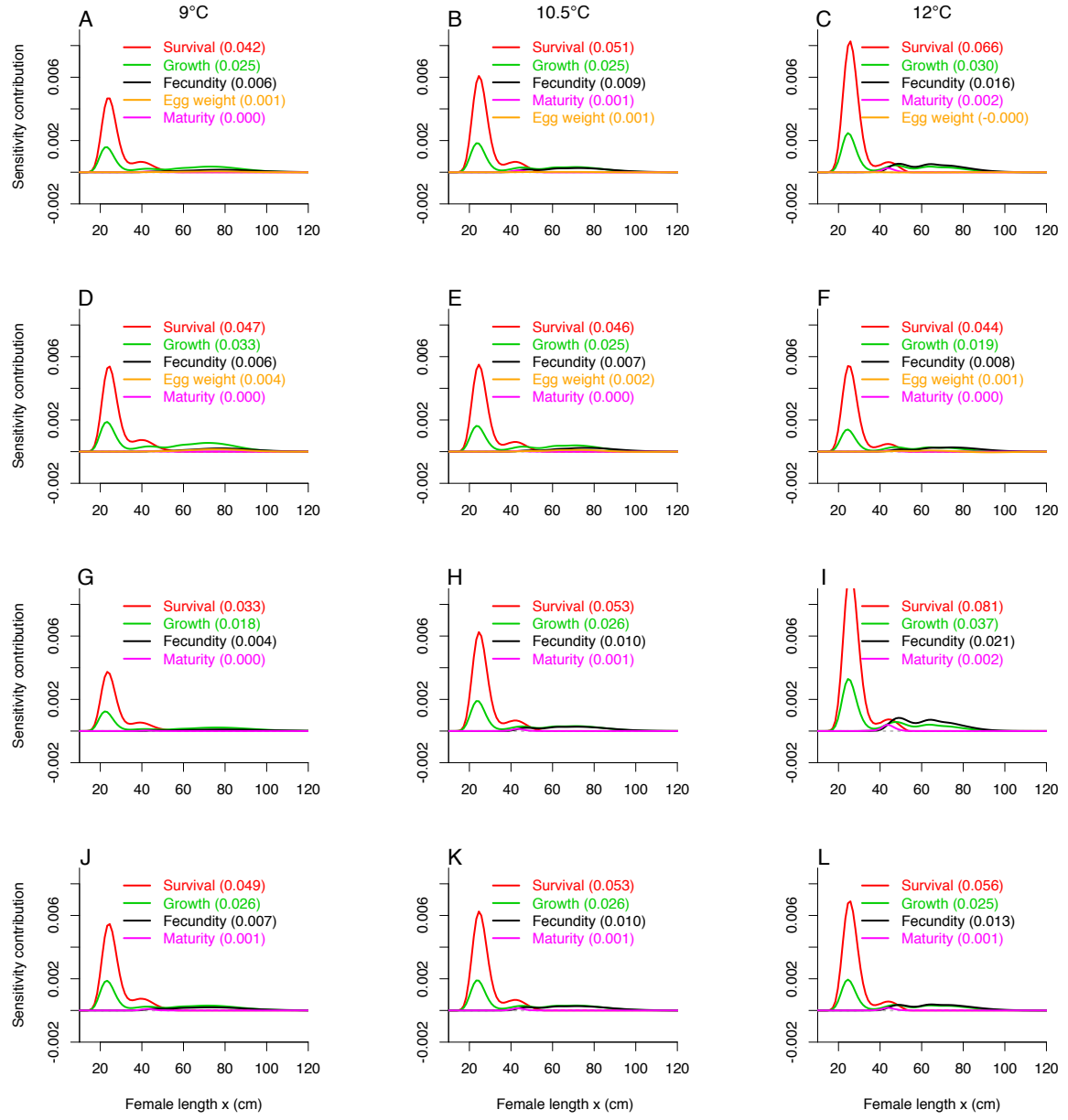


Figure S3.5: Sensitivity results corresponding to the elasticity results in figure S3.4. Sensitivity of λ with respect to female current length x , decomposed into contributions from different vital rates across length x . The sensitivity is evaluated for three different temperatures (Panels A, D, G, J: 9°C; panels B, E, H, K: 10.5°C; and panels C, D, I, L: 12°C), and for four different offspring survival scenarios (panels A, B, C: Scenario 1 Interaction; B, C, D: Scenario 2 Size; G, H, I: Scenario 3 Temperature; and J, K, L: Scenario 4 None). The total sensitivity for each vital rate (integrated over x) is shown in the legends, listed by magnitude of absolute value.

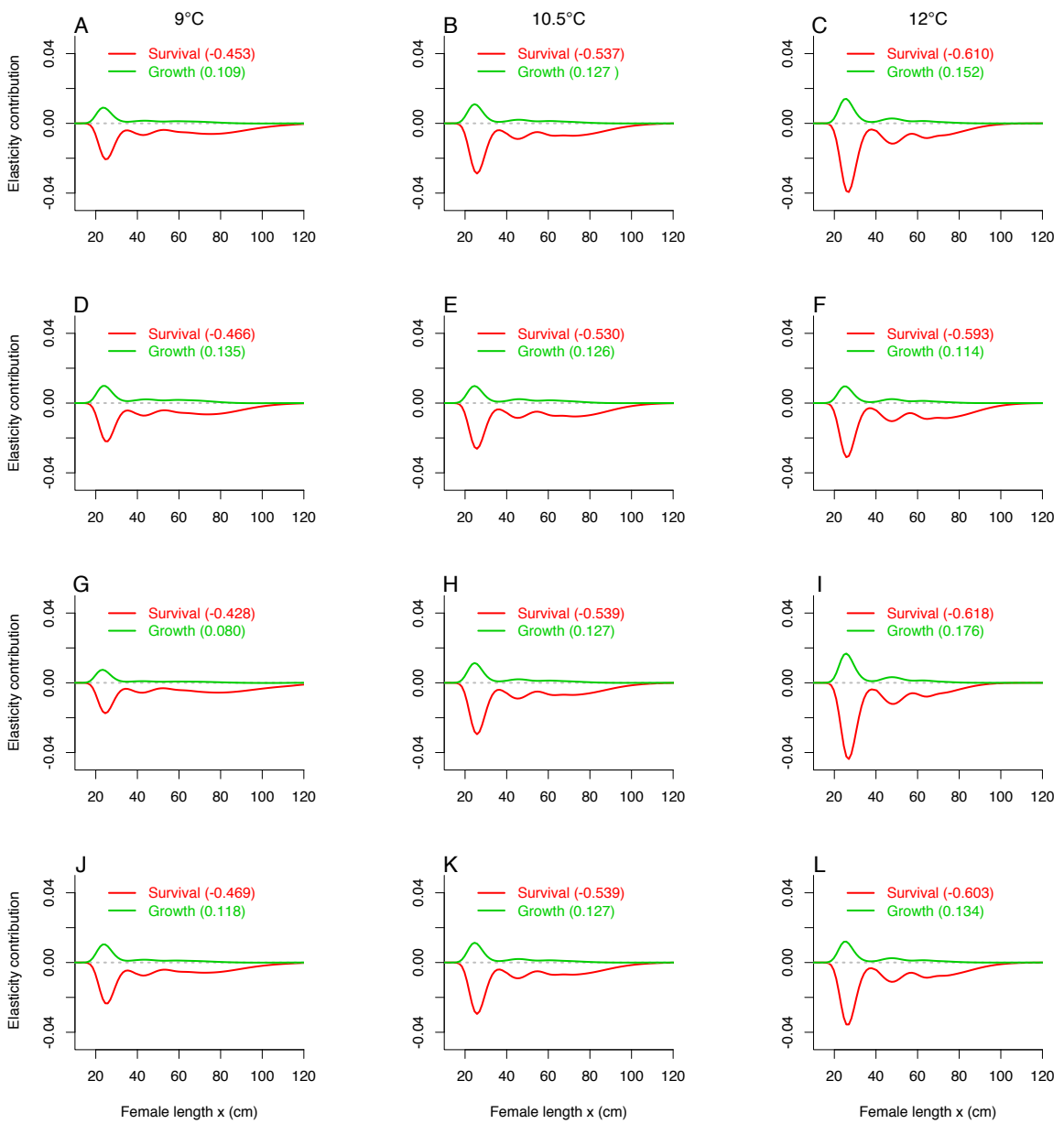


Figure S3.6: Elasticity of λ with respect to female offspring length y , decomposed into contributions from different vital rates across length x . The elasticity is evaluated for three different temperatures (Panels A, D, G, J: 9°C; panels B, E, H, K: 10.5°C; and panels C, D, I, L: 12°C), and for four different offspring survival scenarios (panels A, B, C: Scenario 1 Interaction; B, C, D: Scenario 2 Size; G, H, I: Scenario 3 Temperature; and J, K, L: Scenario 4 None). The total elasticity for each vital rate (integrated over x) is shown in the legends, listed by magnitude of absolute value.

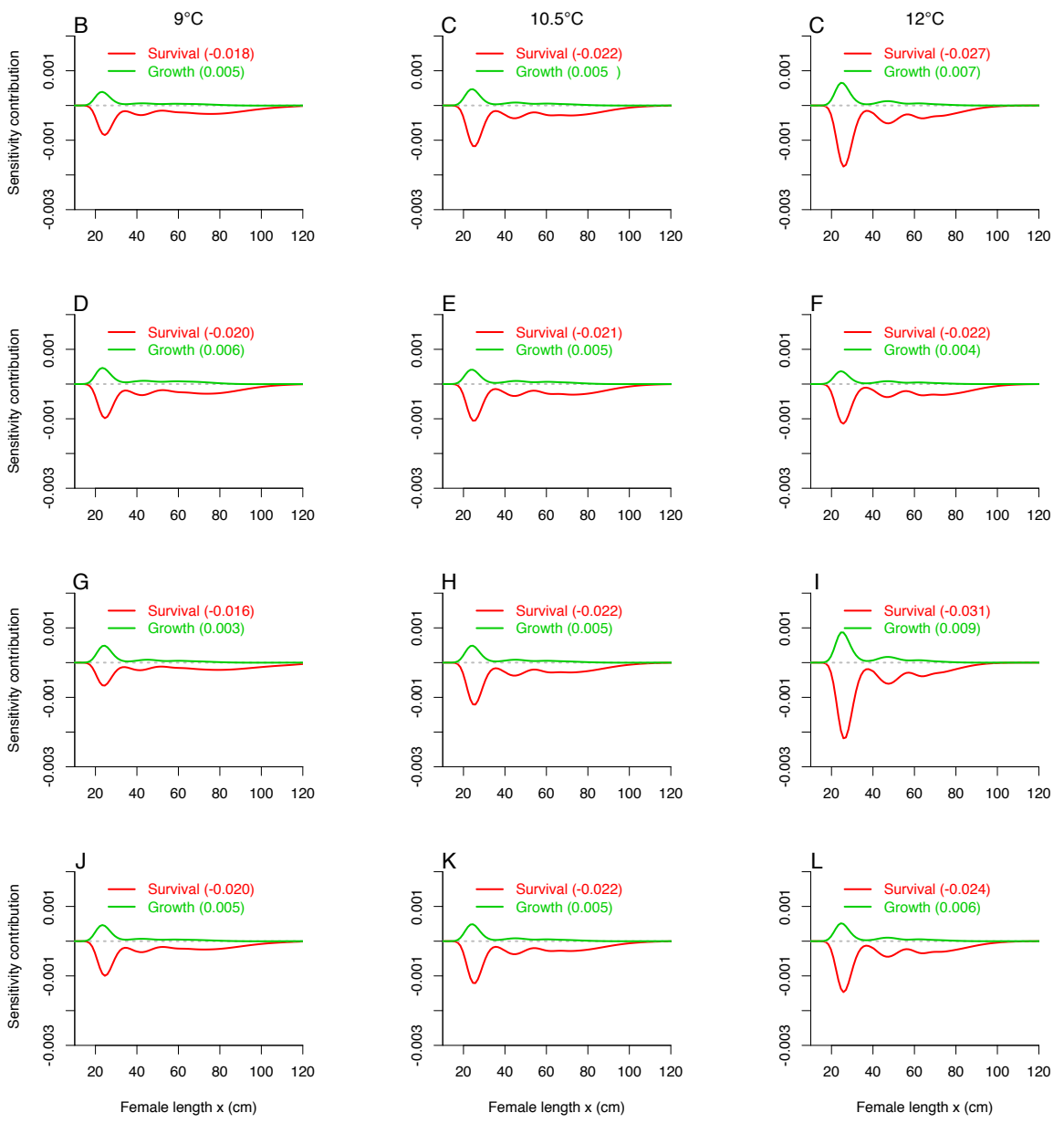


Figure S3.7: Sensitivity results corresponding to the elasticity results in figure S3.6. Sensitivity of λ with respect to female offspring length y , decomposed into contributions from different vital rates across length x . The sensitivity is evaluated for three different temperatures (Panels A, D, G, J: 9°C; panels B, E, H, K: 10.5°C; and panels C, D, I, L: 12°C), and for four different offspring survival scenarios (panels A, B, C: Scenario 1 Interaction; B, C, D: Scenario 2 Size; G, H, I: Scenario 3 Temperature; and J, K, L: Scenario 4 None). The total sensitivity for each vital rate (integrated over x) is shown in the legends, listed by magnitude of absolute value.

S3-4. Elasticities assuming heritability of offspring length

The results presented in the main text are based on a model assuming no heritability in offspring length y (length at age 1), i.e. no correlation between maternal and offspring offspring length at age 1. Here, we evaluate the results for a model including a heritability of 0.3 (slope of relationship between maternal and offspring y , Fig. S3.8). Such a correlation could arise due to genetic inheritance and/or maternal effects. To obtain a comparison model with the same value of λ at the mean temperature of 10.5 °C, the intercept of the parent/offspring regression was reduced accordingly. The variance in offspring length was also reduced in the model including heritability, because some of the variation is now accounted for by parental y (Fig. S3.8).

In this model large offspring will get a fitness advantage not only through increased growth leading to indirect advantages of reproduction and survival, but also because their offspring will in turn tend to grow faster on average than offspring from individuals of smaller offspring length. The elasticity analysis of this model therefore included an extra term corresponding to the elasticity to y in offspring length. This elasticity was positive as expected and quite strong (fig. S3.9). Otherwise, most vital rate elasticities remained similar to those in the main model with no heritability. The elasticity to temperature via offspring length was increased (0.658 vs. 0.483), reflecting the added advantage described above. Corresponding sensitivities are shown in figure S3.10.

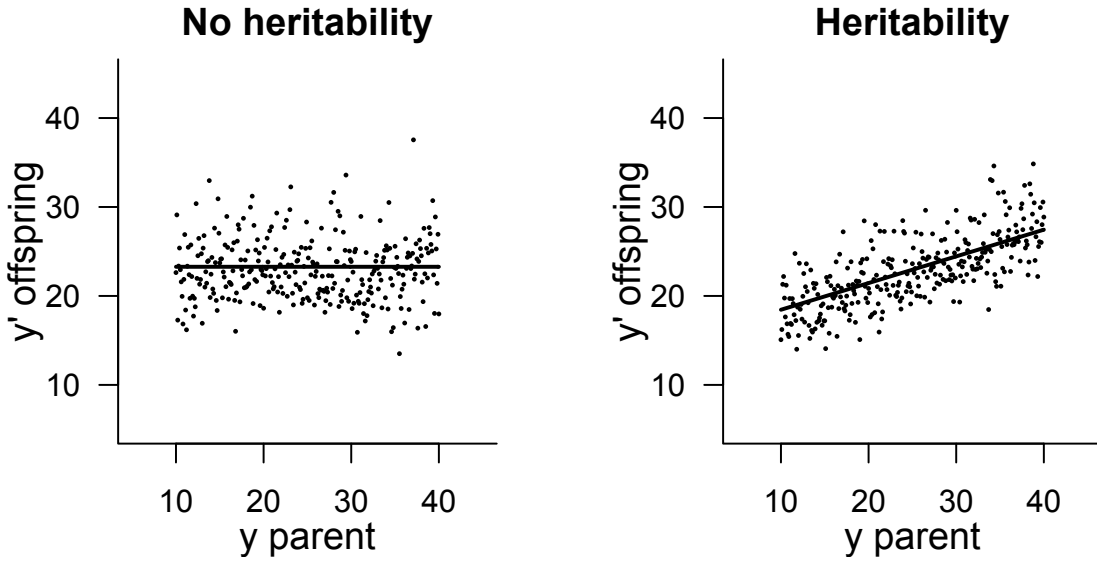


Figure S3.8: Relationship between maternal and (female) offspring offspring length in a model assuming no heritability (left), as in the main text, and with a heritability of 0.3, as used in this appendix. The points are generated from a lognormal distribution with mean and variance according to the corresponding offspring length distribution.

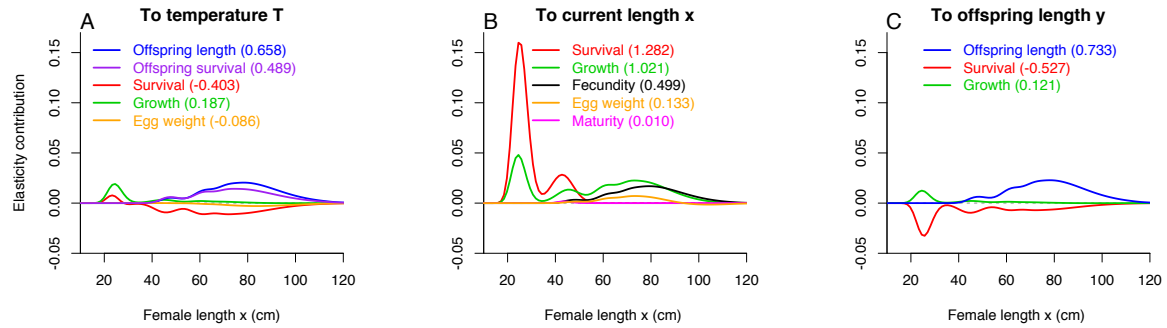


Figure S3.9: Elasticity of λ (calculated for $T = 10.5^{\circ}\text{C}$, using scenario 1 for offspring survival) with respect to temperature T (A), current female length x (B), and female offspring length y (C), decomposed into contributions from each vital rate across x , for a model with heritability of offspring length y (Fig.S3.8). The total elasticity for each vital rate (integrated over x) is shown in the legends, listed by magnitude of absolute value.

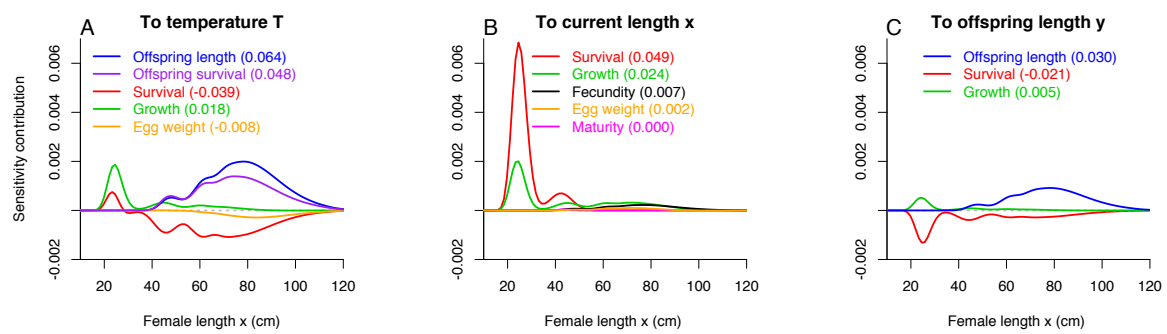


Figure S3.10: Sensitivity of λ (calculated for $T = 10.5^{\circ}\text{C}$, using scenario 1 for offspring survival) with respect to temperature T (A), current female length x (B), and female offspring length y (C), decomposed into contributions from each vital rate across x , for a model with heritability of offspring length y (Fig.S3.8). The total elasticity for each vital rate (integrated over x) is shown in the legends, listed by magnitude of absolute value.

S3-5. Elasticities assuming stronger maternal effect on egg weight

The results presented in the main text apply to a model where the relationship between maternal length and egg weight was leveling off with length, as estimated from the data. A similar pattern has also been shown for other pike populations (Kotakorpi *et al.*, 2013) as well as for other fish species (Kamler, 1992), however it may not be universal. Therefore, we investigated how the elasticity of λ with respect to the maternal length effect on egg size would change if this relationship was linear, and also stronger than in the main model. For this analysis we used scenario 1 (interaction between egg weight and temperature) and scenario 2 (strong effect of egg weight) for offspring survival.

Figure S3.11 shows the alternative linear relationship (red line) between maternal length and egg weight used in this analysis, together with the estimated relationship used in the main model. The slope of the linear relationship corresponds roughly to the maximum slope in the main model (for the smallest length), implying a strong effect of maternal length on egg weight.

Figure S3.12 shows the resulting elasticities for this model (for corresponding sensitivities, see fig. S3.13). Even with these strong assumptions of maternal length effects on offspring survival via egg weight, the elasticity of λ to this effect is still moderate compared to those for survival and growth, although it is substantially higher than in the main model (0.111 vs 0.033 in the main model for offspring survival scenario 1, and 0.570 vs. 0.147 in the main model for scenario 2). For scenario 2 assuming a strong effect of egg weight on offspring survival, this elasticity (and sensitivity) was the highest among all vital rates influencing offspring number, whereas for scenario 1 the elasticity to the length effect on fecundity was still about five times higher. The magnitude of the negative temperature elasticity through egg weight also increases in this model compared to the main model, mediated by

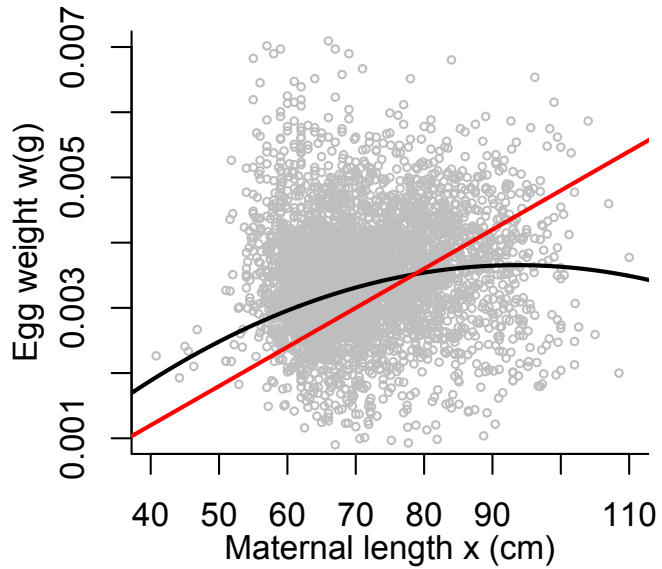


Figure S3.11: Alternative linear relationship between maternal length and egg weight (red line). The black line shows the relationship estimated from data, used in the main model. The alternative model also has a larger slope.

to the stronger effects of maternal length.

Although these results demonstrate that the elasticity of λ to the maternal length effect can be higher under certain strong assumptions (both a strong effect of female length on egg weight and a strong effect of egg weight on offspring survival), we believe that these strong assumptions represent an extreme case. The effect of egg weight on offspring survival is likely smaller in reality than we assumed in scenario 2 (see appendix A4), and the relationship between maternal length and egg weight is much weaker than we assumed in this appendix (at least for pike). Our general conclusion remains that the population growth rate is not sensitive to the maternal length effects on egg weight.

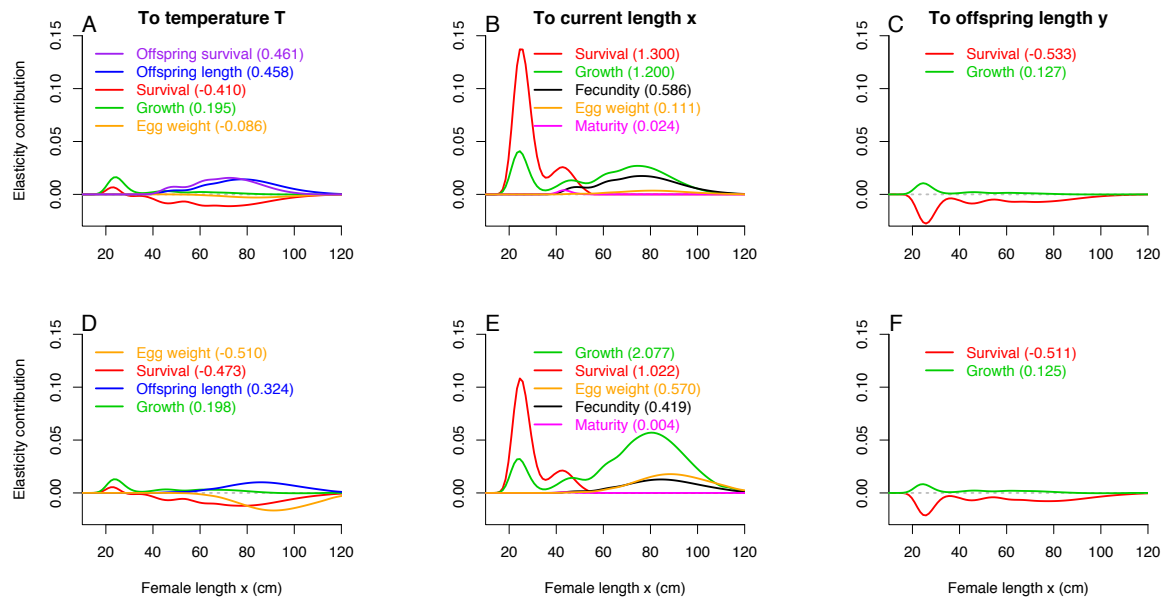


Figure S3.12: Elasticity of λ (calculated for $T = 10.5^\circ\text{C}$) with respect to temperature T (A,D), current female length x (B,E), and female offspring length y (C,F), decomposed into contributions from each vital rate across x , for a model assuming a stronger, linear relationship between maternal length and egg weight (Fig.S3.11). Panels A-C represent calculations using offspring survival scenario 1 (interaction), and panels D-F scenario 2 (size). The total elasticity for each vital rate (integrated over x) is shown in the legends, listed by magnitude of absolute value.

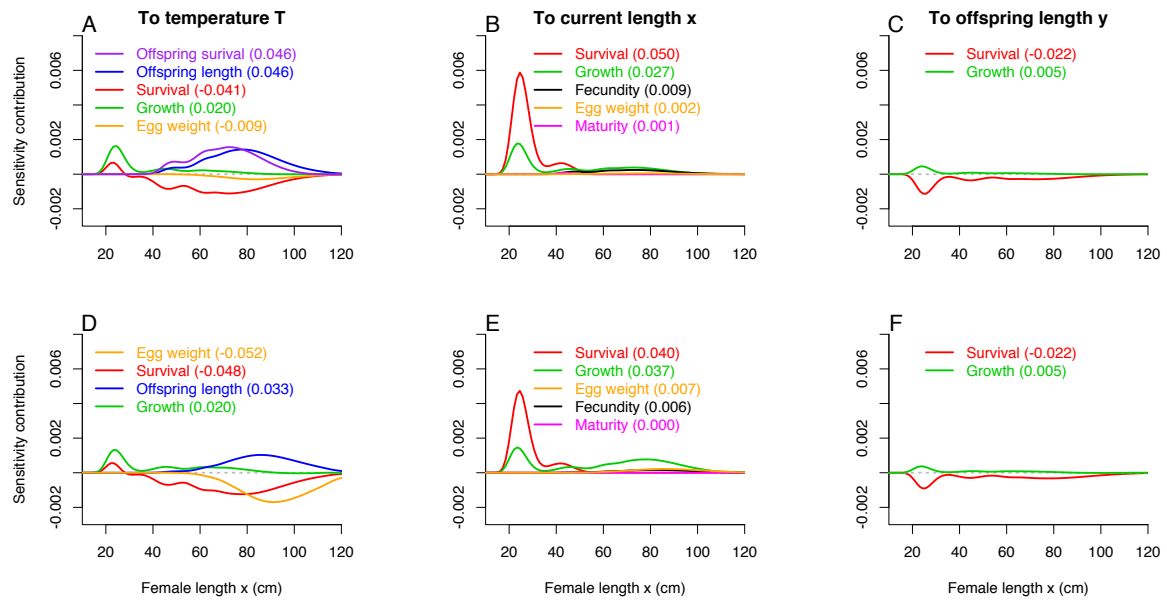


Figure S3.13: Sensitivity of λ (calculated for $T = 10.5^\circ\text{C}$) with respect to temperature T (A,D), current female length x (B,E), and female offspring length y (C,F), decomposed into contributions from each vital rate across x , for a model assuming a stronger, linear relationship between maternal length and egg weight (Fig.S3.11). Panels A-C represent calculations using offspring survival scenario 1 (interaction), and panels D-F scenario 2 (size). The total sensitivity for each vital rate (integrated over x) is shown in the legends, listed by magnitude of absolute value.

References

- Bartoń, K. (2013). *MuMIn: Multi-model inference*.
- Carlson, S.M., Edeline, E., Vøllestad, A., Haugen, T.O., Winfield, I.J., Fletcher, J.M., James, J.B. & Stenseth, N.C. (2007). Four decades of opposing natural and human-induced artificial selection acting on Windermere pike (*Esox lucius*). *Ecol. Lett.*, 10, 512–521.
- Caswell, H. (2001). *Matrix population models*. 2nd edn. Sinauer Associates, Sunderland, Massachusetts.
- Easterling, M.R., Ellner, S.P. & Dixon, P.M. (2000). Size-specific sensitivity: applying a new structured population model. *Ecology*, 81, 694–708.
- Edeline, E., Carlson, S.M., Stige, L.C., Winfield, I.J., Fletcher, J.M., James, J.B., Haugen, T.O., Vøllestad, A. & Stenseth, N.C. (2007). Trait changes in a harvested population are driven by a dynamic tug-of-war between natural and harvest selection. *Proc. Natl. Acad. Sci. U.S.A.*, 104, 15799–15804.
- Ellner, S.P. & Rees, M. (2006). Integral projection models for species with complex demography. *Am. Nat.*, 167, 410–428.
- Frost, W.E. & Kipling, C. (1967). A study of reproduction, early life, weight-length relationship and growth of pike, *Esox lucius* L., in Windermere. *J. Anim. Ecol.*, 36, 651–693.
- Kamler, E. (1992). *Early life history of fish*. Chapman & Hall Fish and Fisheries Series. Chapman & Hall, London.
- Kipling, C. (1983). Changes in the population of pike (*Esox lucius*) in Windermere from 1944 to 1981. *J. Anim. Ecol.*, 52, 989–999.

- Kotakorpi, M., Tiainen, J., Olin, M., Lehtonen, H., Nyberg, K., Ruuhijärvi, J. & Kuparinen, A. (2013). Intensive fishing can mediate stronger size-dependent maternal effect in pike (*Esox lucius*). *Hydrobiol.*, 718, 109–118.
- Langangen, Ø., Edeline, E., Ohlberger, J., Winfield, I.J., Fletcher, J.M., James, J.B., Stenseth, N.C. & Vøllestad, A. (2011). Six decades of pike and perch population dynamics in Windermere. *Fish. Res.*, 109, 131–139.
- Le Cren, E.D. (1951). The length-weight relationship and seasonal cycle in gonad weight and condition in the perch (*Perca fluviatilis*). *J. Anim. Ecol.*, 20, 201–219.
- Merow, C., Dahlgren, J.P., Metcalf, C.J.E., Childs, D.Z., Evans, M.E.K. & Jongejans, E. *et al.* (2014). Advancing population ecology with integral projection models: a practical guide. *Methods Ecol. Evol.*, 5, 99–110.
- Paxton, C., Winfield, I.J., Fletcher, J.M., George, D.G. & Hewitt, D. (2009). Investigation of first year biotic and abiotic influences on the recruitment of pike *Esox lucius* over 48 years in Windermere, U.K. *J. Fish. Biol.*, 74, 2279–2293.
- Pinheiro, J., Bates, D., DebRoy, S., Sarkar, D. & the R Development Core Team (2013). *nlme: Linear and Nonlinear Mixed Effects Models*.
- R Development Core Team (2013). *R: A Language and Environment for Statistical Computing*. R Foundation for Statistical Computing, Vienna, Austria.
- Rees, M., Childs, D.Z. & Ellner, S.P. (2014). Building integral projection models: a user's guide. *J. Anim. Ecol.*, 83, 528–545.
- Vindenes, Y., Edeline, E., Ohlberger, J., Langangen, Ø., Winfield, I.J. & Stenseth, N.C. *et al.* (2014). Effects of climate change on trait-based dynamics of a top predator in freshwater ecosystems. *Am. Nat.*, 183, 243–256.

Vindenes, Y. & Langangen, Ø. (2015). Individual heterogeneity in life histories and eco-evolutionary dynamics. *Ecol. Lett.*, 18, 417–432.

Winfield, I.J., James, J.B. & Fletcher, J.M. (2008). Northern pike (*Esox lucius*) in a warming lake: changes in population size and individual condition in relation to prey abundance. *Hydrobiol.*, 601, 29–40.